



Pomona  
College

SENIOR THESIS IN MATHEMATICS

---

**Simulating Wormhole  
Teleportation and Learning  
Mutual Information on an IBM  
Eagle Processor**

---

*Author:*

Oscar Scholin

*Advisor:*

Professor Ami Radunskaya

Submitted to Pomona College in Partial Fulfillment  
of the Degree of Bachelor of Arts

April 12, 2024

# Contents

<b>1</b>	<b>What is a Quantum Computer?</b>	<b>1</b>
1.1	From the past to the future . . . . .	1
1.2	Review of quantum mechanics . . . . .	3
1.2.1	Let there be light . . . . .	3
1.2.2	Postulates of quantum mechanics . . . . .	4
1.2.3	Spooky action at a distance . . . . .	10
1.3	Connections to computing . . . . .	12
1.3.1	The qubit . . . . .	14
1.3.2	Information space . . . . .	15
1.3.3	The quantum circuit model . . . . .	16
1.4	Variational Quantum Eigensolver . . . . .	18
1.5	Quantum chaos . . . . .	19
1.6	Real life quantum computers . . . . .	21
<b>2</b>	<b>AdS/CFT Correspondence and SYK Hamiltonians</b>	<b>23</b>
<b>3</b>	<b>Simulating Wormhole Dynamics</b>	<b>29</b>
3.1	Simplifying SYK Hamiltonians . . . . .	29
3.1.1	Derivation and characterization of SYK (Sachdev-Ye-Kitaev) Hamiltonian . . . . .	29
3.1.2	Time evolution to simplify? . . . . .	31
3.2	Implementation of rest of wormhole protocol . . . . .	33
3.3	An experiment with a philosophical question . . . . .	43

## Abstract

The quantum computer is the next major revolution in computing, but its development faces many challenges both from theoretical and experimental perspectives. In this thesis, I try to build the simulation environment for wormhole teleportation in the context of Sachdev-Ye-Kitaev (SYK) Hamiltonians from the Anti de-Sitter / Conformal Field Theory (AdS/CFT) correspondence on a quantum computer. In Chapter 1, I review quantum mechanics and the theory of quantum computing. Then in Chapter 2, I give theoretical background in AdS/CFT. Finally, in chapter 3, I give the details of the simulation as well as my results. My motivation to study this topic comes from concerns that [21] have over the recent (November 2022) experiment of this exact process that [19] implemented using Google's Sycamore quantum computer. While the simulation does not produce results completely consistent with established work ([19]), I document and freely publish my code<sup>1</sup> and report real quantum data on a parametrized circuit, as well as offer a path forward for a new way to think about quantum simulations.

---

<sup>1</sup>See <https://github.com/oscars47/Math-Thesis>

# Chapter 1

## What is a Quantum Computer?

“Nature isn’t classical, dammit!” — Richard Feynman

### 1.1 From the past to the future

Possibly the most influential invention in the modern world is the computer. It has taken us to the stars and allowed us to hear gravitational waves; it synthesizes data to learn relationships that would not be possible by hand and enables billions of people daily to interact with each other in a complex, dynamic global economy; it also wakes us up in the morning and distracts us for hours with YouTube and other social media platforms. Imagine if we can change the fundamental way that computing works—we will fundamentally shape not only the way we do science, but the way we understand reality and ourselves and the way we interact with others. To that end, we must consider the physics at hand. The universe is quantum mechanical; therefore, there is an opportunity to use quantum mechanics in how we build our computation systems to take advantage of this framework.

In 1980, Paul Benioff proposed that a computer could operate on the basis of a quantum system [6], as shown in Figure 1.1. In 1981 at a lecture at MIT, physicist Richard Feynman made a bold statement: “The rule of simulation that I would like to have is that the number of computer elements required to simulate a large physical system is only to be proportional to the space-time volume of the physical system.”

Classically, this is not possible. But because of the way quantum mechanics works,

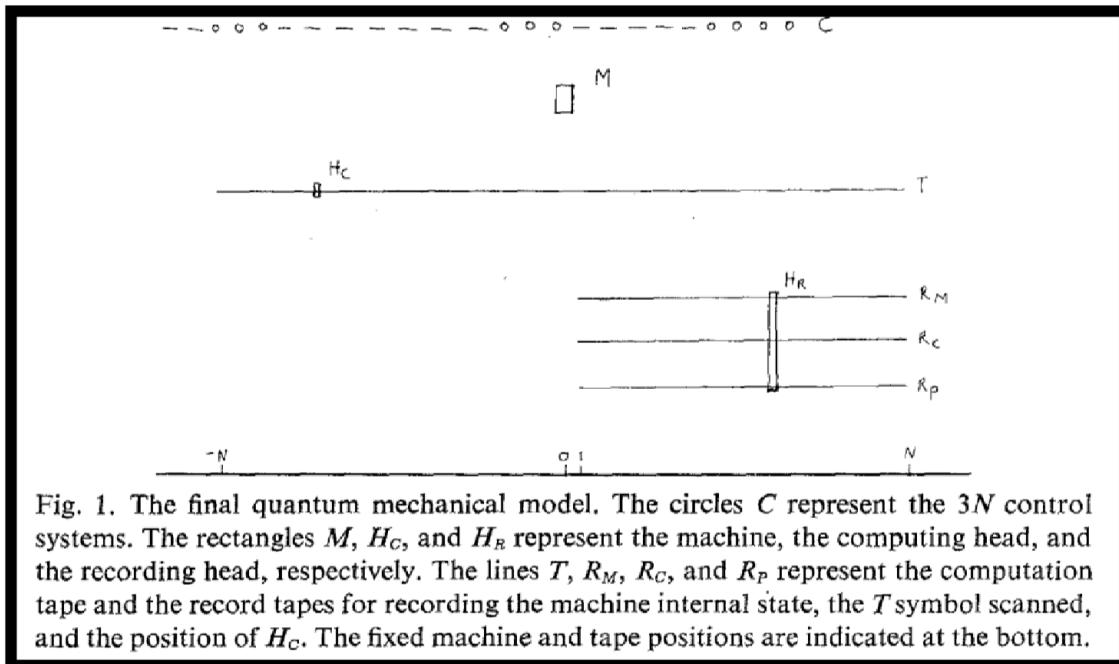


Figure 1.1: The first theoretical model for a quantum computer by Paul Benioff [6].

the information space can grow exponentially with a linear number of “quantum bits”, or “qubits.” We will explain more of the information and computational aspect in section 1.3. The idea is that these two events sparked a revolution in physics and computation that is still in the early-middle stages of development today. This thesis aims to contribute to that development by testing and exploring more efficient ways to implement quantum algorithms.

## 1.2 Review of quantum mechanics

Quantum mechanics is one of the most well-tested and powerful theories in science. It is not merely some esoteric plaything of theoretical physicists: it underpins atomic and molecular structures, led to the development of semiconductors, and has fundamentally changed the way we understand reality.

### 1.2.1 Let there be light

Quantum mechanics has its origin in light. In the late 1800s physicists were working to understand radiation, which is energy given off by some material at a non-zero temperature. Lord Rayleigh and James Jean proposed that the energy of emitted radiation is proportional to the frequency  $\nu$  of the light squared:

$$E = 8\pi kT\nu^2/c^3, \quad (1.1)$$

where  $k$  is Boltzmann’s constant,  $T$  is temperature, and  $c$  is the speed of light [32]. However, as  $\nu = \frac{2\pi}{\lambda}$  increases, i.e. the wavelength  $\lambda$  decreases, bringing the light into the ultraviolet part of the electromagnetic spectrum, the energy  $E$  tends to infinity—this is known as the “ultraviolet catastrophe”. In 1900 Max Planck solved this problem by introducing a strange idea that would forever reshape physics: *quantization*. He proposed that energy, instead of being continuous as was the prevailing theory, comes in discrete packets of size

$$E = \frac{hc}{\lambda} = h\nu, \quad (1.2)$$

where  $h = 6.62607015 \times 10^{-34} \text{ J}\cdot\text{s}$  is Planck’s constant. He derived this relation that every introductory physics and chemistry student learns by considering light as a harmonic oscillator. Classically, this is a sensible model since light, as described by Maxwell’s equations, consists of oscillating electric and magnetic fields perpendicular to each other and the direction of propagation. Moreover, when these oscillating fields

interact with matter, such as electrons in an atom, they can cause the electrons to oscillate in resonance. This oscillation naturally can be modeled as a harmonic oscillator, especially in the limit where the displacements are small and the restoring force is proportional to the distance the particle is displaced.

While Planck initially did not make much fuss over this mathematical trick, Einstein in 1905 illuminated the profound significance of this result by explaining the photoelectric effect [32]. Classically, one would expect that as the intensity of incoming light that hits some surface increases, the average energy carried by an ejected electron should be proportional to this intensity. However, experimentally it was observed to be independent. Einstein's insight was to realize that if instead of thinking of light as a continuous wave, it is actually discrete local packets of energy, then those quanta can be produced or absorbed as a whole. That implies the energy of the released electron is

$$E_{\max} = \frac{hc}{\lambda} - W_0, \quad (1.3)$$

where  $W_0$  is the characteristic energy of the material absorbing the light. These quanta later became known as photons.

### 1.2.2 Postulates of quantum mechanics

With this foundation laid, quantum mechanics began to flourish. Niels Bohr developed the first model of the atom in 1913; de Broglie introduced the wave particle duality by explaining how every object, even a macroscopic one, has a wavelength; in 1925 Werner Heisenberg developed matrix mechanics to describe operators and introduced the uncertainty principle as a consequence of operator non-commutativity; in 1926 Erwin Schrödinger developed the famous Schrödinger equation as well as wave mechanics as an alternative to matrix mechanics; in the 1920s Paul Dirac developed quantum field theory; and in 1935 John von Neumann formalized the mathematics of quantum mechanics by enumerating 5 postulates. From [22], the postulates are:

1. A physical system is described by a Hilbert space  $\mathcal{H}$ , and the state of the system is represented by a ray with norm 1 in  $\mathcal{H}$ .
2. Every physical observable  $A$  corresponds to a self-adjoint (Hermitian) operator  $\hat{A}$  whose eigenvectors form a complete basis.
3. The eigenvalues of  $A$  are the possible measurement outcomes, and the probability of finding the outcome  $a_j$  in a measurement is given by the Born rule:

$$p(a_j) = |\langle a_j | \psi \rangle|^2, \quad (1.4)$$

where  $|\psi\rangle$  is the state of the system and  $|a_j\rangle$  is the eigenstate associated with the eigenvalue  $a_j$  by  $\hat{A}|a_j\rangle = a_j|a_j\rangle$ . If  $a_j$  is  $m$ -fold degenerate, then

$$p(a_j) = \sum_{l=1}^m |\langle a_j^l | \psi \rangle|^2, \quad (1.5)$$

where  $|a_j^l\rangle$  span the  $m$ -fold degenerate subspace.

4. The dynamics of quantum systems is governed by unitary transformations.
5. If a measurement of an observable  $A$  yields an eigenvalue  $a_j$ , then immediately after the measurement, the system is in the eigenstate  $|a_j\rangle$  corresponding to the eigenvalue. This is called *measurement*.

While a full discussion of these postulates is beyond the scope of this chapter, we can discuss some important implications. The first postulate introduces the notion of a Hilbert space, which is the vector space in which all states live. Importantly, the state is a ray of norm 1. The norm 1 is central because this reflects that states are inherently probabilistic (see postulate 3). The fact it is a ray implies that the overall orientation, i.e. complex phase, does not matter. Let us illustrate both points. Consider the state  $|\psi\rangle$  written in Dirac bra-ket notation[26] in the standard basis. Note that the “bra”  $\langle |$  refers to the left pointing chevron, and the “ket”  $| \rangle$  the right. Note that  $| \rangle = \langle |^\dagger$ , where the dagger  $\dagger$  represents the adjoint or complex conjugate transpose. The ket is a column vector, and the bra is a row vector. Consider the example 2-level state

$$|\psi\rangle = \frac{1}{\sqrt{2}} (|0\rangle - |1\rangle). \quad (1.6)$$

with  $|0\rangle = \begin{bmatrix} 1 \\ 0 \end{bmatrix}$  and  $|1\rangle = \begin{bmatrix} 0 \\ 1 \end{bmatrix}$ . This state is a *superposition* of the  $|0\rangle$  and  $|1\rangle$  states. The Born rule for finding state value implies that if we can construct a device to act as an operator that measures  $|0\rangle$  and  $|1\rangle$ , then the probability of finding  $|\psi\rangle$  in state  $|0\rangle$  is given by taking the modulus squared of the inner product of  $|0\rangle$ ,  $|1\rangle$  with  $|\psi\rangle$ .

$$|\langle 0 | \psi \rangle|^2 = \frac{1}{2} \quad (1.7)$$

$$|\langle 1 | \psi \rangle|^2 = \frac{1}{2}. \quad (1.8)$$

$$(1.9)$$

We see that the relative phase of  $e^{i\pi}$  disappeared when we compute the probabilities of measurement in the  $|0\rangle$ ,  $|1\rangle$  basis. We can also rewrite the state in a different basis:

$$|+\rangle = \frac{1}{\sqrt{2}} (|0\rangle + |1\rangle), \quad |-\rangle = \frac{1}{\sqrt{2}} (|0\rangle - |1\rangle):$$

$$|\psi\rangle = |-\rangle, \quad (1.10)$$

hence

$$|\langle +|\psi\rangle|^2 = 0 \quad (1.11)$$

$$|\langle -|\psi\rangle|^2 = 1. \quad (1.12)$$

$$\quad \quad \quad (1.13)$$

We see the basis of the states tell us the probability amplitude for measuring that particular element of the basis, be it  $|0\rangle$  or  $|1\rangle$  or  $|+\rangle$  or  $|-\rangle$ . To be more mathematically concrete, we need to consider the 2nd postulate. To measure in the  $|0\rangle, |1\rangle$  basis, we consider the operator  $I$ :

$$I|0\rangle = |0\rangle \quad (1.14)$$

$$I|1\rangle = |1\rangle, \quad (1.15)$$

i.e.  $I$  is the identity operator

$$I = \begin{bmatrix} 1 & 0 \\ 0 & 1 \end{bmatrix}. \quad (1.16)$$

All operators that correspond to physical observables must be Hermitian in order that their eigenvalues, the quantities we would actually measure in the lab, are real. Moreover, its eigenstates must form a complete basis for the system.

A key idea in quantum mechanics is the uncertainty principle [31]: that is, it is not possible to have complete information about all aspects of a state simultaneously. For example, consider the position operator  $\hat{x}$  and momentum  $\hat{p}$ . These act on an arbitrary state  $|\phi(x)\rangle$  as follows:

$$\hat{x}|\phi\rangle = x|\phi\rangle \quad (1.17)$$

$$\hat{p}|\phi\rangle = -i\hbar \frac{d}{dx}|\phi\rangle. \quad (1.18)$$

The commutator in general is

$$[\hat{A}, \hat{B}] = \hat{A}\hat{B} - \hat{B}\hat{A}, \quad (1.19)$$

hence

$$[\hat{x}, \hat{p}] = \hat{x}\hat{p} - \hat{p}\hat{x}. \quad (1.20)$$

When acting upon  $|\phi\rangle$ ,

$$\begin{aligned} [\hat{x}, \hat{p}]|\phi\rangle &= x(-i\hbar \frac{d}{dx}|\phi\rangle) + i\hbar \frac{d}{dx}(x|\phi\rangle) \\ &= -ix\hbar(\frac{d}{dx}|\phi\rangle) + i\hbar|\phi\rangle + ix\hbar \frac{d}{dx}|\phi\rangle \\ &= i\hbar, \end{aligned} \tag{1.21}$$

where  $\hbar = \frac{h}{2\pi}$  is the reduced Planck's constant. While it is beyond the scope of this chapter to prove this, note that because  $\hat{x}$  and  $\hat{p}$  are conjugate variables, i.e. they are Fourier transforms of each other, they satisfy the above relation [31]. The commutator is deeply linked to uncertainty. If we have two operators, their uncertainty relation is:

$$\Delta\hat{A}\Delta\hat{B} \geq \frac{1}{2}|[\hat{A}, \hat{B}]|. \tag{1.22}$$

Thus the famous Heisenberg relation is

$$\begin{aligned} \Delta\hat{x}\Delta\hat{p} &\geq \frac{1}{2}|[\hat{x}, \hat{p}]| \\ &\geq \frac{\hbar}{2}. \end{aligned} \tag{1.23}$$

The fourth postulate is incredibly significant because it describes the fundamentals of dynamics in a quantum system: they must be unitary, which is a consequence of the conservation of probability. Consider a state  $|\phi(x, 0)\rangle$  at some time  $t = t_1$ . At some later time  $t_2$ , the state will evolve according to unitary dynamics:

$$|\phi(x, t_2)\rangle = \hat{U}(t_2 - t_1)|\phi(x, t_1)\rangle, \tag{1.24}$$

where  $\hat{U}(t)$  is the time evolution operator.  $\hat{U}(t)$  must be generated from some Hermitian operator, so suppose

$$\hat{U}(t) = e^{-\frac{i}{\hbar}\hat{H}t}. \tag{1.25}$$

$\hat{H}$  is a special operator because it must have units of energy (J); we therefore associate it with the energy of the state (the argument can be made more rigorous, but this will suffice for now). Consider an infinitesimal shift in time  $dt$  and Taylor expand

the exponential:

$$\begin{aligned}
|\phi(x, t + dt)\rangle &= e^{-\frac{i}{\hbar} \hat{H} dt} |\phi(x, t)\rangle \\
&= (1 - \frac{i}{\hbar} \hat{H} dt + \dots) |\phi(x, t)\rangle \\
&\approx (1 - \frac{i}{\hbar} \hat{H} dt) |\phi(x, t)\rangle \text{ to first order since } dt \text{ is small} \\
\therefore |\phi(x, t)\rangle + dt \frac{d}{dt} |\phi(x, t)\rangle &\approx (1 - \frac{i}{\hbar} \hat{H} dt) |\phi(x, t)\rangle \\
\therefore \hat{H} |\phi(x, t)\rangle &= \frac{i}{\hbar} \frac{d}{dt} |\phi(x, t)\rangle,
\end{aligned} \tag{1.26}$$

which is the time dependent Schrödinger's equation, the governing equation of motion in a quantum system!<sup>1</sup>

The last we will say about the postulates is to touch on the complexity of "measurement." Earlier we said we can compute the probability a state is in a given basis state by using the Born rule. But what actually would we do in the lab to make that measurement? And if we measure, what happens to the quantum state? Postulate 5 states that "immediately after measurement, the system is in the eigenstate  $|a_j\rangle$  corresponding to the measured eigenvalue  $a_j$ . There are several interpretations of what actually happens to the quantum state, but the most common one is the notion of "collapse": that the state has been forced to choose from among its possible superpositions in an irreversible (and hence non-unitary) transformation [4]. This is what we observe experimentally.

In Figure 1.2, we show the famous double-slit experiment, in which there is some incident source that hits a wall with two openings, and then finally reaches a second wall [31]. If we had classical particles, like tennis balls, then the observed pattern on the screen would be random. If we have a wave, then interference between the part of the wave that goes through the first slit with the part that goes through the second creates an interference pattern, places of light and dark stripes on the wall. With a quantum particle, the curious thing is that the observed pattern reflects not a classical particle but a wave! This strange behavior reflects superposition: the particle effectively went through both slits simultaneously, hence the observed interference is actually self-interference. But there is a twist: if the particle is observed *before* it can pass through the slits, the pattern is now random. That is, the act of observing changed the state itself. As far as what an "observation" or "measurement" must

---

<sup>1</sup>However, this is not relativistic. Paul Dirac later solved this problem, but we will be working in the non-relativistic limit so the Schrödinger equation is acceptable.

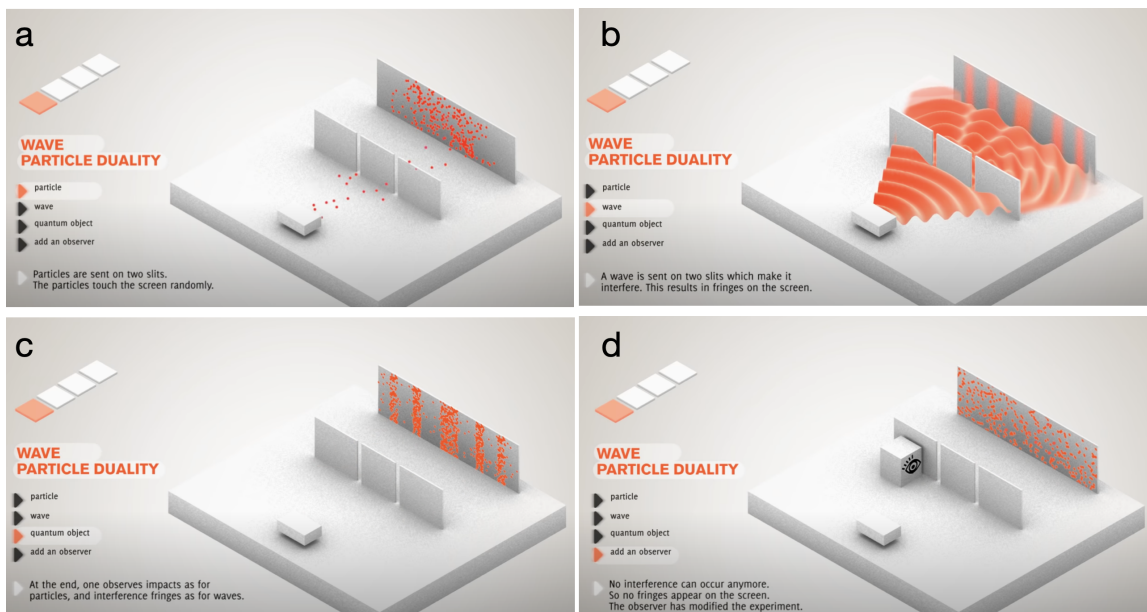


Figure 1.2: Simulation of double slit experiment for classical particles (a), waves (b), quantum particles (c), and observed quantum particles (d). From <https://toutestquantique.fr/en/duality/>.

actually consist of, though the figure implies some kind of eye “watched” the particles, there is no need for consciousness or other human involvement. A simple beam of light will suffice. The point is to somehow cause an interaction with the quantum particle that causes state collapse. This happens naturally in a process called *decoherence*, whereby a quantum state will lose its “quantum” nature by collapsing to an eigenstate after enough interaction with the environment. Exactly what about the interaction or disturbance is needed to cause the collapse is in general not known [31]. For any kind of experiment involving quantum processes, especially computing, preventing decoherence is a key issue.

### 1.2.3 Spooky action at a distance

Another other very interesting, counter-intuitive, and important feature of quantum mechanics is *entanglement*. Mathematically, a state  $|\phi\rangle$  is entangled if it is not possible to separate it as a product of states:

$$|\phi\rangle \neq |\phi_1\rangle \otimes |\phi_2\rangle, \quad (1.27)$$

where the tensor product  $\otimes$  denotes how we combine two quantum states into one shared Hilbert space. As an example, consider the 2 dimensional Bell states:

$$|\Phi^+\rangle = \frac{1}{\sqrt{2}} (|00\rangle + |11\rangle) \quad (1.28)$$

$$|\Phi^-\rangle = \frac{1}{\sqrt{2}} (|00\rangle - |11\rangle) \quad (1.29)$$

$$|\Psi^+\rangle = \frac{1}{\sqrt{2}} (|01\rangle + |10\rangle) \quad (1.30)$$

$$|\Psi^-\rangle = \frac{1}{\sqrt{2}} (|01\rangle - |10\rangle). \quad (1.31)$$

None of these states can be factored in the form of Equation 1.27 since there are necessarily cross terms from the tensor product that are missing in the Bell states. These states are also interesting because they are *perfectly entangled*: they are completely non-separable. In my physics thesis I prove a new theoretical result about these kinds of states in high dimension; they are of deep interest to quantum algorithms and communication protocols.

Physically, what entanglement between some number of particles—not restricted only to a pair—means is that information is stored in the *correlations* between the particles and cannot be solely resolved in the individual particles themselves. This

leads to the paradox where if I have an entangled pair of particles and keep one in my lab but send the other one to Venus, if I measure my particle the state of the other one must *instantaneously* update.<sup>2</sup> Before anyone worries about causality breaking, we note that no information is actually transferred in this process; it exists in the wavefunction of the state, and moreover I cannot force the particle I have in my lab to collapse to a value I decide I want with absolute certainty, so I cannot use entanglement to perform faster than light communication. Nonetheless, it is still non-trivial and intriguing.

Einstein, Podolsky, and Rosen (EPR) first brought up the possibility of entanglement in 1935 [11]. In 1964, John Bell provided a mathematical framework to test the notion of a “local hidden variables theory” that Einstein and others favored as an alternative explanation of quantum mechanics: essentially, the universe is in fact deterministic, not probabilistic as quantum mechanics would suggest, we simply do not have the knowledge of “hidden variables” that act on a local scale and could explain the results of our experiments perfectly [5]. Bell formulated a mathematical way to quantify the strength of classical correlations versus quantum correlations, which is also physically feasible to test—the upper bound for the classical case is known as Bell’s inequality. To “violate” the inequality, that means to observe greater correlation than is explainable classically.

In 1982, a group led by Alain Aspect was the first to violate Bell’s inequality experimentally conclusively, building off of the work by John Clauser, using entangled photons generated from a decaying calcium-40 atom [3]. Their setup is shown in Figure 1.3: the radioactive source emits entangled photons in two directions; these photons are separated by a polarizing beam splitter (the cube with a line through it), such that the photon goes one way if it is a “ $|0\rangle$ ” (horizontally polarized) and another if it is “ $|1\rangle$ ” (vertically polarized). This allows us to apply operations to rotate the polarization state with the polarimeter (P.M.) in order to project the state into different bases other than “ $|0\rangle$ ” and “ $|1\rangle$ ”. We can measure the “single” counts of particles with a single photon detector, and we can also measure the “coincidence” counts of particles detected by the singles counter within a given time window (typically on the order of nanoseconds). These coincidence counts—for example, how often we detect a particle vertically polarized on the right given the one on the left was also vertically polarized—are what go into Bell’s inequality. Aspect with this setup violated the classical limit by about 46.5 standard deviations, which is almost ten times the amount needed to claim a scientific discovery.

---

<sup>2</sup>Scientists, like Jian-Wei Pan, have actually performed measurements of entangled states separated over 1200 kilometers using satellites [33]!

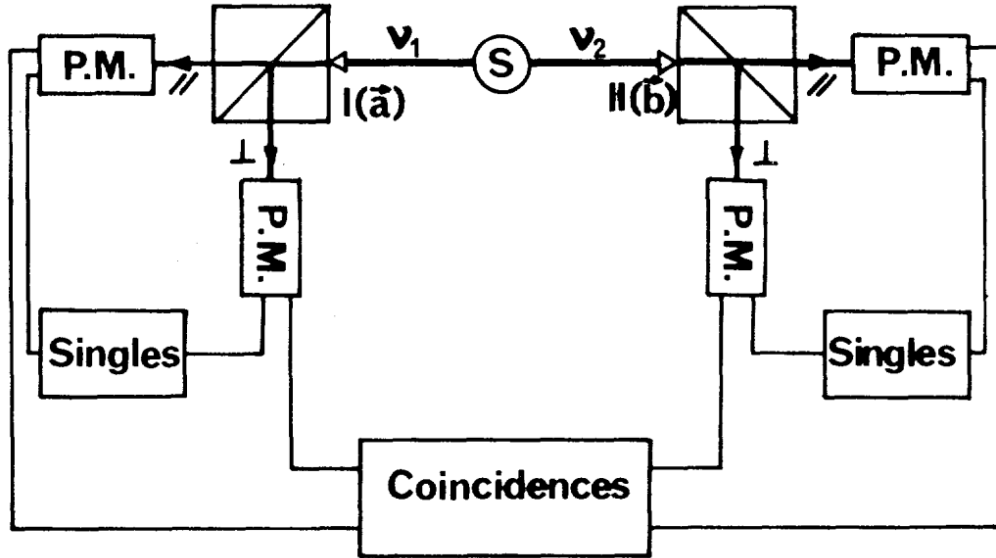


Figure 1.3: Experimental setup from Alain Aspect’s lab which was the first to violate Bell’s inequality [3]. P.M. stands for polarimeter, which rotate the polarization state of light to allow for projection of the state into different bases.

To get a better sense of the physical process involved in this experiment, consider Figure 1.4, produced by a group of scientists in Vienna including Anton Zeilinger. Conceptually, their setup is quite similar to that of Aspect, although instead of using a decay process they use a process called Spontaneous Parametric Downconversion that uses a nonlinear crystal to “split” incoming photons from a laser into entangled pairs. The crucial thing to observe is that only the photons on the left panel of each separate snapshot had their polarization rotated by changing the angle of a waveplate, but the photons on the right panel also respond. While this behavior could represent merely correlations, the fact that this relationship persists despite any permutation of local basis proves that it is in fact non-trivial, quantum behavior—entanglement. The reason we see “clouds” of photons is that these images are the result of several seconds worth of data measured by a CCD compiled together.

### 1.3 Connections to computing

Now that we have an understanding of the basics of quantum mechanics, let us explore the intersection with computing. David Deutsch, one of the founders of

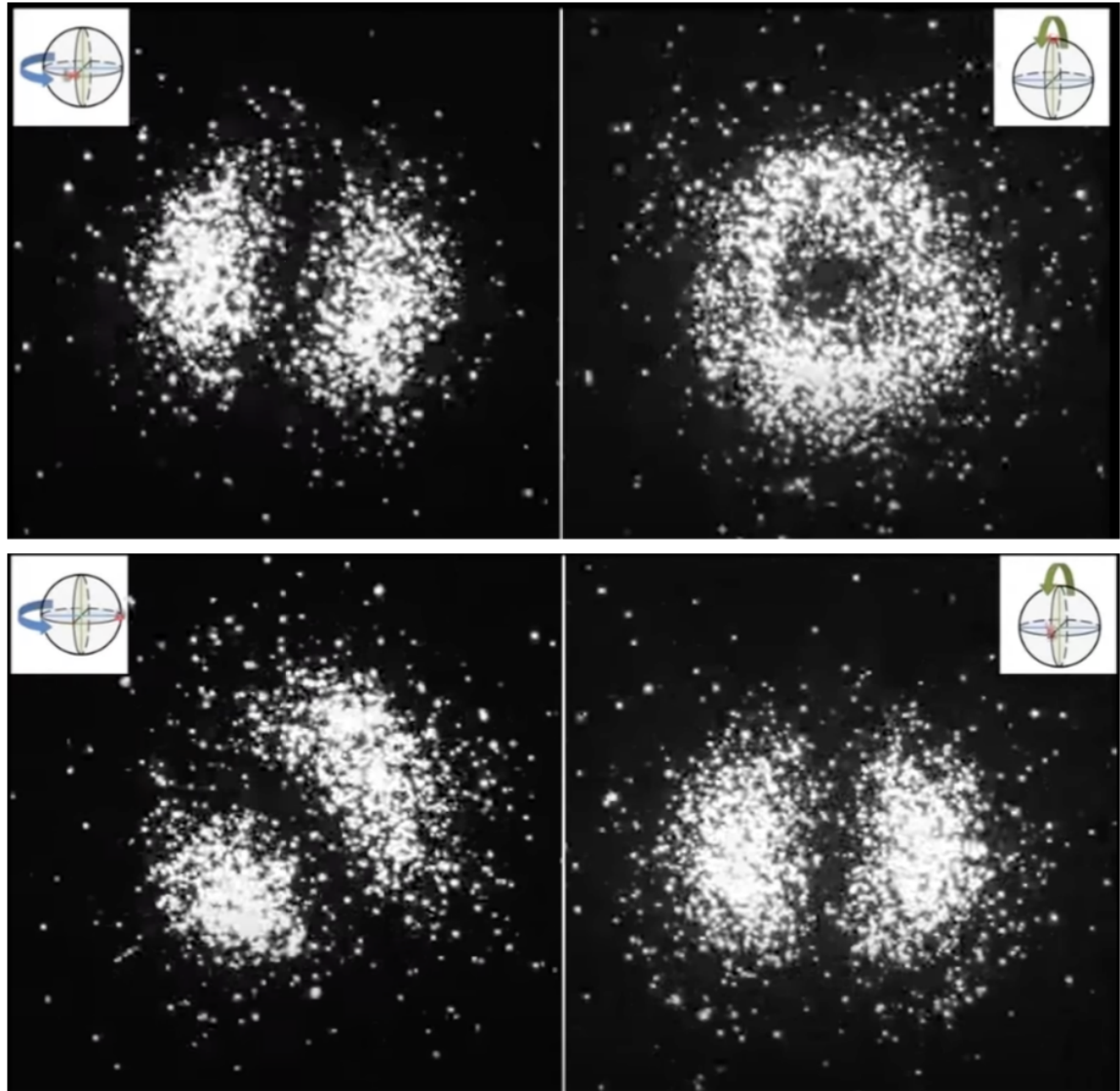


Figure 1.4: Two snapshots from [https://youtu.be/wGkx1MUw2TU?si=GQ\\_ifWdoEAdJiIk0](https://youtu.be/wGkx1MUw2TU?si=GQ_ifWdoEAdJiIk0) which are visualizations of entanglement. Only the idler photons (left image) basis measurement is changed, yet the trigger photons also respond.

quantum algorithms, aptly explains the heart of the connection, which comes almost out of necessity:

“It is argued that underlying the Church–Turing hypothesis there is an implicit physical assertion. Here, this assertion is presented explicitly as a physical principle: ‘every finitely realizable [SIC] physical system can be perfectly simulated by a universal model computing machine operating by finite means’. Classical physics and the universal Turing machine, because the former is continuous and the latter discrete, do not obey the principle, at least in the strong form above. A class of model computing machines that is the quantum generalization of the class of Turing machines is described, and it is shown that quantum theory and the ‘universal quantum computer’ are compatible with the principle.” [10]

The Church-Turing thesis is a crucial concept in computer science, which proposes that a function is computable if and only if it can be evaluated by a Turing machine. A Turing machine is a theoretical computer that consists of an infinite string of tape upon which symbols can be manipulated using a set of rules. There is an implicit assertion when we consider the Church-Turing thesis from a physical perspective: the processes governing the physical world, as long as they can be finitely described and result in finite outcomes, should be simulatable by a Turing machine using finite means [28]. However, because classical physics is continuous and deterministic, it cannot be perfectly simulated by traditional computing machines, which operate discretely and with finite resources. Fluid simulation is a prime example of the limitations of classical computation: such elegant, natural processes become a nightmare to solve mathematically.

By contrast, quantum mechanics is discrete—its eponymous hallmark is quanta. This, as Deutsch points out, makes a universal quantum computer a natural choice of a finite Turing Machine. Moreover, while it sounds like a trivial statement, it is profoundly true: nature is quantum; therefore, to model natural processes, we need a *quantum* not *classical* computer.

### 1.3.1 The qubit

A qubit is the quantum analog of a bit. Whereas a bit can only exist as either a 0 or a 1, a qubit is in a superposition of 0 and 1:

$$|\phi\rangle = \alpha|0\rangle + \beta|1\rangle, \quad (1.32)$$

where  $\alpha, \beta \in \mathbb{C}$  such that  $|\alpha|^2 + |\beta|^2 = 1$ . Superposition allows a system of  $n$  qubits to represent a superposition of all  $2^n$  possible states simultaneously. We can represent

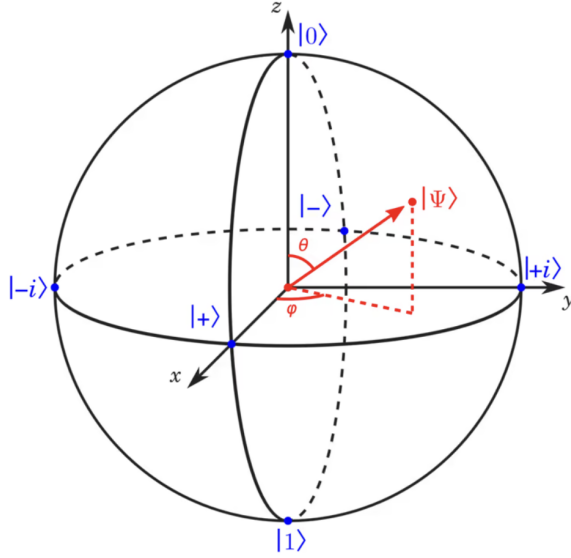


Figure 1.5: The Bloch sphere, from <https://prefetch.eu/know/concept/bloch-sphere/>.

these states as existing on the surface of the *Bloch sphere*, shown in Figure 1.5. Up to this point, the states I have written out have been *pure states*, in that they have definite representation in terms of some basis. We can have a more general *mixed state*, which is a classical probabilistic mixture of different states:

$$|\Phi\rangle = \sum_i p_i |\phi_i\rangle, \quad (1.33)$$

where each  $|\phi_i\rangle$  is a pure state.

### 1.3.2 Information space

In this subsection we elaborate on the gain in information space using quantum computation as opposed to classical. By “information space” we mean the range or domain of possible information states that a system can represent or process.

For a classical computer, the information space grows linearly with the number of bits. Adding one more bit doubles the size of the information space. Any operation on classical bits explores this space sequentially, one state at a time.

For a quantum computer, due to superposition, the information space grows exponentially with the number of qubits. This is not limited to the number of available

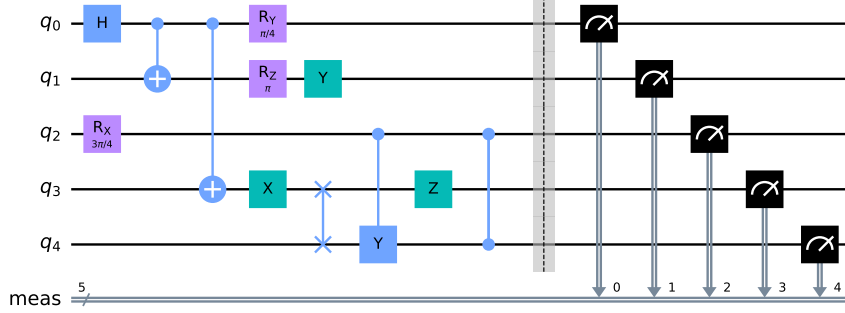


Figure 1.6: Example quantum circuit.

states, but also the number of states that can be explored.

While it might seem initially that entanglement could reduce the information space due to the correlated nature of entangled particles, it actually enhances the complexity and potential of quantum information processing: as stated earlier, there can be more information than just what is stored in the particles themselves individually. Moreover, since entanglement has no classical counterpart, it allows for operations and algorithms that are not possible with binary logic; there is therefore an incoming paradigm shift in the basic logic of computers.

### 1.3.3 The quantum circuit model

Now that we have the basic motivation for quantum computers, let us explain some important formalism, using the conventions explained in [26]. Consider Figure 1.6. We call this a *quantum circuit*. Each line represents a qubit. There are single and multi-qubit operations; these are the boxes and circles. The circuit begins with all states in the *ground state*. That means, the total state of the circuit, or register, looks like:

$$|0\rangle \otimes |0\rangle \otimes |0\rangle \otimes |0\rangle \otimes |0\rangle. \quad (1.34)$$

The computation proceeds in *moments*: notice the operations are aligned in columns; all the operators in a register are applied simultaneously. The most common operators, also called gates, are the ones I have included on the circuit. The Hadamard

gate is:

$$H = \frac{1}{\sqrt{2}} \begin{bmatrix} 1 & 1 \\ 1 & -1 \end{bmatrix}. \quad (1.35)$$

The Pauli  $X, Y, Z$  gates are:

$$X = \begin{bmatrix} 0 & 1 \\ 1 & 0 \end{bmatrix}, \quad (1.36)$$

$$Y = \begin{bmatrix} 0 & -i \\ i & 0 \end{bmatrix} \quad (1.37)$$

$$Z = \begin{bmatrix} 1 & 0 \\ 0 & -1 \end{bmatrix}. \quad (1.38)$$

The Pauli  $X, Y, Z$  rotations are:

$$R_X(\theta) = \begin{bmatrix} \cos \frac{\theta}{2} & -i \sin \frac{\theta}{2} \\ -i \sin \frac{\theta}{2} & \cos \frac{\theta}{2} \end{bmatrix}, \quad (1.39)$$

$$R_Y(\theta) = \begin{bmatrix} \cos \frac{\theta}{2} & -\sin \frac{\theta}{2} \\ -\sin \frac{\theta}{2} & \cos \frac{\theta}{2} \end{bmatrix}, \quad (1.40)$$

$$R_Z(\theta) = \begin{bmatrix} e^{-i\lambda/2} & 0 \\ 0 & e^{i\lambda/2} \end{bmatrix}. \quad (1.41)$$

$$(1.42)$$

The two qubit gates we consider are mostly conditional, meaning the operation applied to one of the qubits, called the *target*, is dependent on the other *control* qubit. The most common are control  $X$  (CNOT), control  $Y$ , control  $Z$ . The control gates are simple: if the value of the control is 1, apply  $X/Y/Z$ , if 0, then do nothing. They are especially interesting if the control is in a superposition. Then complex entangled states can be created. For example, if a Hadamard gate is applied to the control and then a CNOT, we create the  $|\Phi^+\rangle$  state:

$$\text{CNOT}(H \otimes I)(|0\rangle \otimes |0\rangle) = \text{CNOT} \frac{1}{\sqrt{2}}((|0\rangle + |1\rangle) \otimes |0\rangle) = \frac{1}{\sqrt{2}}(|00\rangle + |11\rangle), \quad (1.43)$$

where we have adopted the shorthand notation that  $|a\rangle \otimes |b\rangle = |ab\rangle$ . The only non-conditional two qubit gate of interest to us is the SWAP gate, whereby two qubits are physically moved to swap places. Then we can perform measurement in any basis, as the speed-dial looking device indicates.

There is a central idea in the quantum circuit model called the *Universal Gate Theorem* [9]. With a *universal gate set*, any other gate of set size can be constructed. The most common set from a theoretical perspective is,

$$\{R_X, R_Y, R_Z, \text{CNOT}\}. \quad (1.44)$$

I.e., the single qubit rotation gates and the two-qubit CNOT can be used to implement a gate in a quantum circuit of an arbitrary size of Hilbert space  $d = 2^n$ . The exact representation of the gates will differ depending on the physical implementation of the quantum computer. The point is now we have the mathematical framework to construct more complicated algorithms.

## 1.4 Variational Quantum Eigensolver

The current era of quantum computing is NISQ, or noisy-intermediate stage quantum computing [28]. The “noisy” refers to the fact that the operations we perform on our qubits are not perfectly accurate; in other words, we have not yet developed in real time error correction, which is an essential part of computing. Therefore, of interest in the meantime are *hybrid* algorithms that utilize both quantum and classical processing. The variational quantum eigensolver (VQE) is one such algorithm.<sup>3</sup>

The main idea of a VQE is quite simple [7]. Say I have some Hamiltonian  $\hat{H}$  (as in Equation 1.26), which is represented as a sum of tensor products of Pauli matrices typically denoted as Pauli strings, e.g.:

$$\hat{H} = \alpha XYZZ + \beta YYZZ + \gamma XXZ \quad (1.45)$$

where  $\alpha, \beta, \gamma$  are complex scalars and  $X, Y, Z$  are the Pauli matrices given in Equations 1.36, 1.37, 1.38 with implicit tensor products between them in order to reflect separate actions on distinct qubits. Note that they must all have the same size, or else we assume implicitly there are extra identity terms. For example, the last term in the sum really refers to  $XXZI$ . Let us assume we have already determined the form of  $\hat{H}$ . The problem a VQE tries to answer is how do we create a circuit to determine the lowest eigenvalue of the Hamiltonian  $\hat{H}$ , which corresponds to the ground state energy of the system.

---

<sup>3</sup>See <https://learning.quantum.ibm.com/tutorial/variational-quantum-eigensolver> for documentation on coding a VQE in Python, which is what I use to present the results in Chapter 4.

There is no known direct way to determine the optimal circuit a priori, so we use a heuristic method. First, we create an *ansatz* or an educated guess of the form the circuit must have, in that we specify the collection of gates in a certain order to create the circuit we believe will find the ground state. Say I have prepared the state  $|\psi\rangle$  in my circuit so far. Then, we want to find the parameters to the ansatz in order to minimize the expectation value  $\langle\psi|\hat{H}|\psi\rangle$ . We can view this as a gradient descent optimization problem with the loss function as the expectation value. We use a classical computer to estimate the gradients by using the quantum computer to evaluate the loss function.

The beauty of this approach is that we use the quantum computer to do what is difficult classically—simulating Hamiltonians—but use a classical computer to evaluate gradients. VQEs have a great deal of applicability to optimization problems in general: if one can make the ground state of a Hamiltonian the solution, a VQE will find it [12, 1].

## 1.5 Quantum chaos

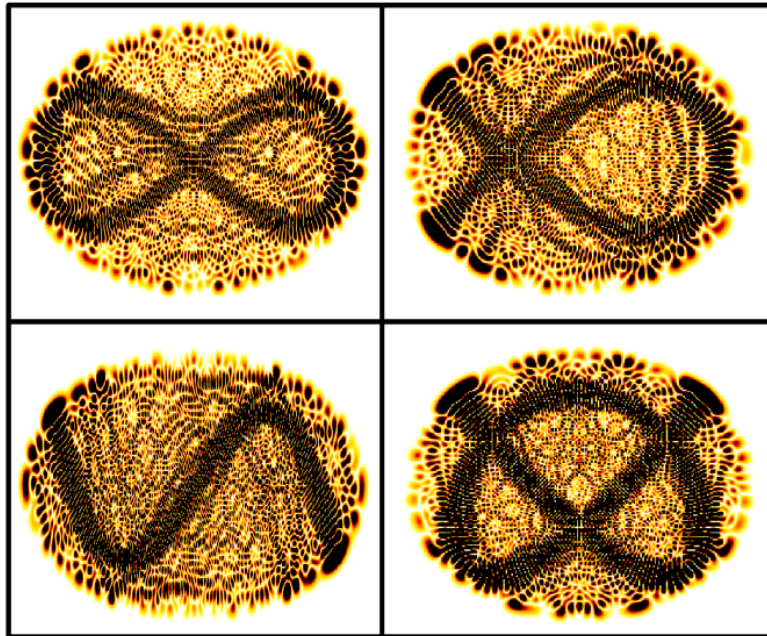


Figure 1.7: Sample plots of quantum Lissajous scarring from [20].

Quantum chaos is the study of quantum phenomena with connections to classical

systems with chaotic dynamics [29]. While a full literature review in this area is beyond the scope of this chapter, I describe the main metric of interest for this paper as well as point out some cool examples worth further investigation.

Central to the problem of this thesis is *mutual information*, which quantifies the amount of entanglement entropy between two qubits, here  $P$  and  $T$ . It is defined as

$$I_{PT} = S_P + S_T - S_{PT}, \quad (1.46)$$

for  $S_X = -\text{Tr}(\rho_X \ln \rho_X)$ , where  $\rho_X$  is the reduced density matrix corresponding to subsystem  $X$ . The density matrix of a quantum state  $|\psi\rangle$  is

$$\rho = |\psi\rangle\langle\psi|. \quad (1.47)$$

To obtain the reduced form of this matrix, we perform a partial trace operation over the other qubits not  $X$  [26]. This allows us to isolate a qubit or qubits of interest. The partial trace for a matrix  $A \otimes B$  is:

$$\text{Tr}_A(A \otimes B) = \text{Tr}(A)B, \quad \text{Tr}_B(A \otimes B) = A \text{Tr}(B). \quad (1.48)$$

Let us go through an example to illustrate how to calculate the partial trace. Say we have a 2-level system with a density matrix

$$\rho = \begin{bmatrix} \rho_{11} & \rho_{12} & \rho_{13} & \rho_{14} \\ \rho_{21} & \rho_{22} & \rho_{23} & \rho_{24} \\ \rho_{31} & \rho_{32} & \rho_{33} & \rho_{34} \\ \rho_{41} & \rho_{42} & \rho_{43} & \rho_{44} \end{bmatrix}. \quad (1.49)$$

Then the reduced density matrix of the first subsystem is

$$\rho_1 = \text{Tr}_2(\rho) = \begin{bmatrix} \rho_{11} & \rho_{13} \\ \rho_{31} & \rho_{33} \end{bmatrix} + \begin{bmatrix} \rho_{22} & \rho_{24} \\ \rho_{42} & \rho_{44} \end{bmatrix} = \begin{bmatrix} \rho_{11} + \rho_{22} & \rho_{13} + \rho_{24} \\ \rho_{31} + \rho_{42} & \rho_{33} + \rho_{44} \end{bmatrix}, \quad (1.50)$$

and the reduced density matrix of the second subsystem is

$$\rho_2 = \text{Tr}_1(\rho) = \begin{bmatrix} \rho_{11} & \rho_{12} \\ \rho_{21} & \rho_{22} \end{bmatrix} + \begin{bmatrix} \rho_{33} & \rho_{34} \\ \rho_{43} & \rho_{44} \end{bmatrix} = \begin{bmatrix} \rho_{11} + \rho_{33} & \rho_{12} + \rho_{34} \\ \rho_{21} + \rho_{43} & \rho_{22} + \rho_{44} \end{bmatrix}. \quad (1.51)$$

If we have a Hamiltonian that describes a quantum ‘chaotic’ system, then under time evolution we might observe the mutual information to behave in characteristic manner. I am vague here because unlike in classical mechanics, where we can talk

about the notion of trajectories and positive Lyapunov exponents to quantify the sensitivity to initial conditions, there is less of a clear-cut definition [29]. This is primarily due to the facts that: trajectories cannot exist due to the Heisenberg uncertainty principle (as established above) and the solutions to the Schrödinger equation are stable. In fact, as [29] states, “Quantum chaos, or wave chaos, is a study of the signatures of classical chaos of the underlying classical dynamical system”—so it mainly appears in the context of comparing quantum analogs of classical systems. Figure 1.7 demonstrates a quintessential example of quantum chaos known as *scarring*, whereby the quantum probability density is increased in a region that corresponds to a classical periodic orbit. The authors of [20] demonstrate how scars resembling Lissajous curves emerge in the eigenstates of a perturbed two-dimensional anisotropic harmonic oscillator.

In this thesis, as we will see in the next chapter, we are primarily interested in simulating a particular quantum system which has a signature information transfer as a function of time, so mutual information will be our key metric, without as much of a rigorous focus on “quantum chaos” per se.

## 1.6 Real life quantum computers

There are several major companies (IBM, Google, Amazon, Rigetti, D-Wave, Xanadu, IonQ)<sup>4</sup> pursuing one the main approaches to implementing quantum computers in real life, which are: superconducting electrons, trapped ions, neutral atoms, and quantum optics [15]. While explaining the physics of these different methods is beyond the scope of this thesis, I want to highlight the first one: superconducting electrons, also called SQUIDs, and in particular on IBM. IBM is probably the most advanced company in quantum computing both for their pioneering work in building the largest and best performing SQUID systems, which include up to 1121 qubits on the Heron processor, as well as for the amount of effort to create a software environment to develop quantum algorithms and interface with their real processors and simulators in the cloud though their Python package `Qiskit`.<sup>5</sup>

As of Spring 2024, anyone can access IBM’s Eagle series processors, which have 127 qubits, for free<sup>6</sup> using the IBM Quantum Experience: <https://quantum.ibm.com/>.

---

<sup>4</sup>See <https://www.forbes.com/sites/technology/article/top-quantum-computing-companies/?sh=55d594d73a94> for a more complete list.

<sup>5</sup>See <https://www.ibm.com/quantum/blog/eagle-quantum-processor-performance> for more information regarding IBM’s processor.

<sup>6</sup>Up to 10 minutes of compute time per month.

The IBM quantum computers do not have built in error correction—like all other current quantum computers—but it is possible to run error mitigation. I discuss this and more of the nuances of executing my custom-built algorithm on a real IBM Eagle processor (specifically, on the Kyoto unit) in Chapter 4.

Before discussing the details of the simulation that the code I wrote attempts to implement, I note that the IBM quantum computers use a different universal gate set than the one I mentioned before due to the physical nature of the system. In particular, their set is:

$$\{\text{ECR}, R_X, X, \sqrt{X}\}, \quad (1.52)$$

which are defined as 1) the echo cross-resonance gate<sup>7</sup>

$$\text{ECR} = \frac{1}{\sqrt{2}}(IX - XY) = \frac{1}{\sqrt{2}} \begin{bmatrix} 0 & 1 & 0 & i \\ 1 & 0 & -i & 0 \\ 0 & i & 0 & 1 \\ 0 & i & 0 & 1 \\ -i & 0 & 1 & 0 \end{bmatrix}, \quad (1.53)$$

which is maximally entangling and is equivalent to a CNOT up to single qubit rotations. 2) and 3) have the same definition as before, and 4)<sup>8</sup>

$$\sqrt{X} = \frac{1}{2} \begin{bmatrix} 1+i & 1-i \\ 1-i & 1+i \end{bmatrix}. \quad (1.54)$$

We can interpret  $\sqrt{X}$  as rotating the state in  $x$ -direction by  $\frac{\pi}{2}$ , which is half of the  $\pi$  rotation of the  $X$  gate.

---

<sup>7</sup><https://docs.quantum.ibm.com/api/qiskit/qiskit.circuit.library.ECRGate>

<sup>8</sup><https://docs.quantum.ibm.com/api/qiskit/qiskit.circuit.library.SXGate>

# Chapter 2

## AdS/CFT Correspondence and SYK Hamiltonians

We have established a basic understanding of quantum mechanics, the connections to computing, and that real-life quantum computers exist. In order to get to the point where we can discuss the details of how to simulate wormhole teleportation on a quantum computer, we need to take a step back and give a high-level overview of what this process entails.

The AdS/CFT correspondence is a proposed relationship between a 2-dimensional model of gravity, the Anti-de sitter space, and 1-dimensional quantum conformal field theory [17]. This thesis investigates a particular physical example of the AdS/CFT correspondence: a spin Hamiltonian of Majorana fermions, the Sachdev-Ye-Kitaev (SYK) model, that describes the interactions between these particles in large clouds, which can be employed in a quantum circuit to model a time-evolution process mathematically equivalent to a particle traversing an Einstein-Rosen bridge between two black holes [13]. In this chapter, I will focus primarily on rigorously defining the SYK Hamiltonian.

While a rigorous description of AdS/CFT, which is derived from a string theory framework, is beyond the scope of this section, it is worth discussing for a bit. AdS, the Anti de Sitter space, is a  $2d$  general relativistic model of gravity for a universe with negative curvature, so spacetime is conceived as hyperbolic as opposed to spherical, if it had positive curvature, or flat, if it had 0 curvature; the sign of the curvature is based on the mass density of the universe, which is still a topic physicists are debating [17]—see Figure 2.2 for a visual of the curvatures. On the

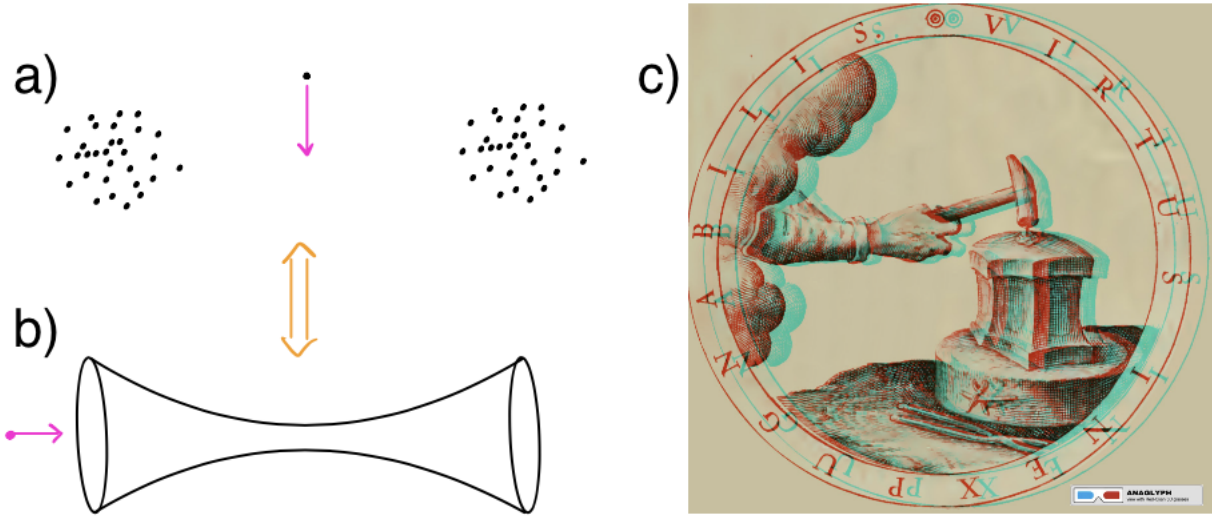


Figure 2.1: a) and b) demonstrate the AdS/CFT correspondence: a) shows a system of two clouds of quantum particles, which are made to interact as another particle (pink arrow) is injected into the system (conformal field theory); b) shows a system holographically dual system in a gravitation setting (AdS), in which the event horizons of two black holes are connected by an Einstein-Rosen bridge, which a particle traverses. c) shows an example of a hologram, in which 3-dimensional information is encoded on a 2-dimensional surface. This is a visual way of understanding the relationship between the AdS model of gravity and QFT: the AdS is like the "hologram" that emerges from the encoding in QFT.

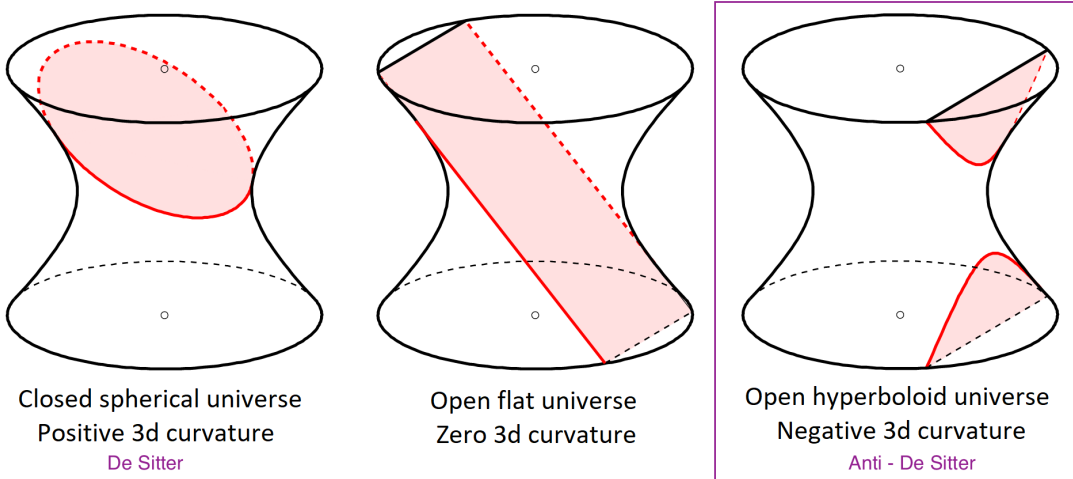


Figure 2.2: Comparison of different models of gravity and their corresponding curvatures, from <https://physics.stackexchange.com/questions/353148/is-de-sitter-space-with-non-zero-curvature-an-acceptable-model-for-the-universe>.

other hand, we have CFT, or conformal field theory. Our current understanding of the universe at the most elementary level, given by the Standard Model of Particle Physics, is based on quantum field theory: that is, that the fundamental object in the universe is a field [27]. All the elementary particles we observe are quantized excitations of their field, much like waves on the surface of a pond. This means that these disturbances must come in discrete packets, a fundamental idea in quantum mechanics [27]. The conformal descriptor reflects that the field theory is unaffected by conformal operations, which are transformations, rotations, dilations, and the like—in other words, gauge invariance. We limit ourselves to 1 d theories.

I want to employ a mathematical and a physical metaphor I think will be helpful to intuitively understanding the basis of the equivalence of these two ideas, which admittedly seem pretty distinct. Consider an orientable manifold  $\Omega$  and a differential form  $\omega$ . By the General Stokes Theorem, we know

$$\int_{\Omega} d\omega = \int_{\partial\Omega} \omega. \quad (2.1)$$

In other words, the “volume” integral over the entire manifold  $\Omega$  of the derivative of the  $\omega$  is equivalent to the “surface” integral of  $\omega$  over the boundary of  $\Omega$ . That is, all the “information” we can learn by considering the entire manifold in fact resides on

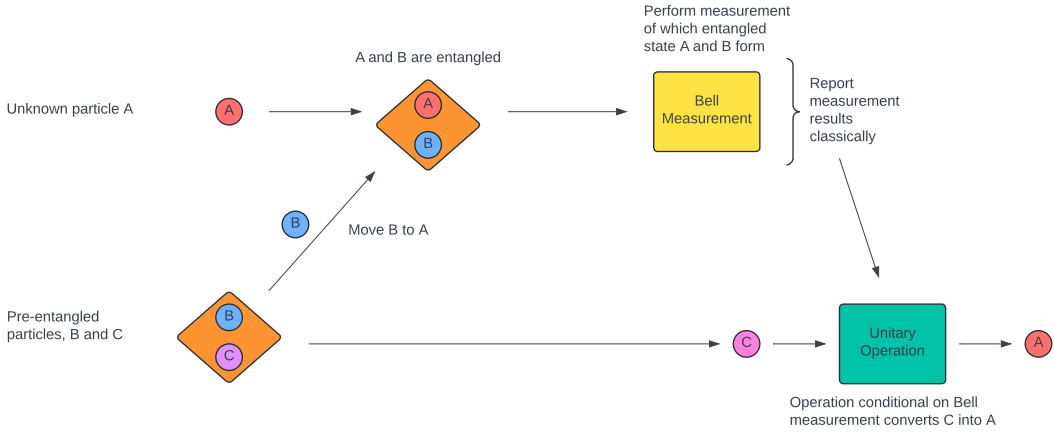


Figure 2.3: An illustration of quantum teleportation. Initially two qubits are entangled and then spatially separated. An unknown state is entangled with one of the originally entangled pair, which now extends the entanglement across the threesome. This new pair is measured with respect to a basis of completely entangled states (aka the Bell basis, which my physics thesis focuses on in more detail by investigating a kind of approximation to a quantum computer using only linear operations); based on this measurement, a classical signal is transmitted, and an operation is performed on the remaining original state that teleports the unknown state to where the old state had been. Note that there is nothing suspicious here, since a classical signal is required, and so causality is not violated.

the surface. In this same way, we can imagine AdS as  $\Omega$  and CFT as  $\partial\Omega$ : actually this entire theory of gravity is encoded mathematically within this quantum field theory, just bumped up one dimension. Or consider a physical example: a 3D Anaglyph, as shown in Figure 2.1 c), is a 3D image formed from the superposition of red and cyan 2D images—the entire description of the system is reducible to a lower dimension, but both represent fundamentally the same thing.

To the specific model at hand, we are interested in a system of two clouds of  $N$  particles, as shown in Figure 2.1 a). Ultimately what happens is we inject a new particle into the system, which, because of existing entanglement between the clouds, induces a series of interactions by which the information content of the particle (which I will define more explicitly shortly) becomes completely chaotically scrambled and then spontaneously reassembles itself at the end of the protocol—that is, mathematically

just a more complicated version of quantum teleportation, which I walk through in Figure 2.3). However, this is equivalent in a higher dimensional gravitational space to a particle traversing a wormhole, or an Einstein Rosen bridge [19]. Before too much doubt settles in about “wormholes”, let me make an important statement: according to general relativity,

$$E^2 = m^2 + p^2 \quad (2.2)$$

where  $m$  is an object’s rest mass and  $p$  is the magnitude of its relativistic momentum. Thus  $E > 0$  always. This constraint renders an Einstein-Rosen bridge between two event horizons untraversable [19]. However, in quantum field theory, there is a kind of particle called a virtual particle, and quantum fluctuations allow for pairs of virtual particles to spontaneously create and then annihilate each other—a classical example is Hawking radiation [16]. In order to conserve energy, one of the pairs has positive energy, and the other has negative energy. Therefore negative energy can exist within a QFT perspective. Thus, if we simulate this gravitational traversal in a quantum system, the wormhole in fact becomes traversable in the dual equivalent.

The single most important object in this thesis is the SYK Hamiltonian, which we use in Schrödinger’s equation to determine the time evolution of the system as discussed in Chapter 1. The SYK model is defined as [19, 25, 24]:

$$\hat{H} = \sum_{i < j < k < l}^{N_m} \mathcal{J}_{i,j,k,l} \psi_i \psi_j \psi_k \psi_l, \quad (2.3)$$

Let us unpack this equation.  $\mathcal{J}_{i,j,k,l}$  is some scalar coupling constant drawn from a Gaussian distribution with  $\mu = 0$  and  $\sigma^2 = \frac{J^2 3!}{N_m^3}$ . Each of the four  $\psi$  are quantum states; in particular, Majorana fermions. We present them as matrices. Thus the multiplication between the particle states as shown above is just matrix multiplication. Here,  $N_m$  are the number of particles, which we require to be even. Majorana fermions are half-integer spin particles that must satisfy

$$\psi = \psi^*, \quad (2.4)$$

where  $*$  denotes the anti-particle (and really what we should be thinking is it means the Majorana fermion field is real, which simplifies calculations nicely) [27]. These states are relevant to consider because of how they appear in 2D materials like graphite [2]. Equation 2.4 implies

$$\{\psi_i, \psi_j\} = \delta_{i,j}, \quad (2.5)$$

where the curly brackets denote the anti-commutator,  $\{A, B\} = AB - BA$ , and

$$\delta_{i,j} = \begin{cases} 1 & \text{if } i = j \\ 0 & \text{else,} \end{cases}$$

is the Kronecker delta. It turns out Equation 2.5 is the definition of Clifford Algebra, so we can find mathematical objects that satisfy this relation and are useful to us. In particular, we are interested in matrices since the operator formalism of quantum mechanics uses the language of linear algebra. Ultimately, we want to convert from a fermionic system to a qubit system, which is the framework for quantum computation, which is the focus of the next chapter.

# Chapter 3

## Simulating Wormhole Dynamics

### 3.1 Simplifying SYK Hamiltonians

#### 3.1.1 Derivation and characterization of SYK (Sachdev-Ye-Kitaev) Hamiltonian

In this chapter I describe the details of the wormhole teleportation protocol as well as how I am simulating it in Python. All code used to implement the simulation as well as run hardware is located at my Github repository.<sup>1</sup> We use IBM's Qiskit package for constructing and measuring the quantum circuits. The code is the result of trying to interpret the protocol based on the information available in [19]. Several questions remain to be addressed and are discussed in the following sections.

We write the SYK Hamiltonians for either the L or R blackhole, hereafter termed simply the subsystem L or R with  $N_m$  Majorana fermions each. We expand Equation 2.3 as

$$\hat{H}_{L,R} = \sum_{p=0}^N H_{p_{L,R}} \quad (3.1)$$

$$= \sum_{i=0}^{N_m-1} \sum_{j=i+1}^{N_m-1} \sum_{k=j+1}^{N_m-1} \sum_{l=k+1}^{N_m-1} \mathcal{J}_{ijkl} \psi_{L,R}^i \psi_{L,R}^j \psi_{L,R}^k \psi_{L,R}^l \quad (3.2)$$

---

<sup>1</sup>[https://github.com/oscar47/Math-Thesis/blob/main/syk\\_qk\\_redo.py](https://github.com/oscar47/Math-Thesis/blob/main/syk_qk_redo.py)

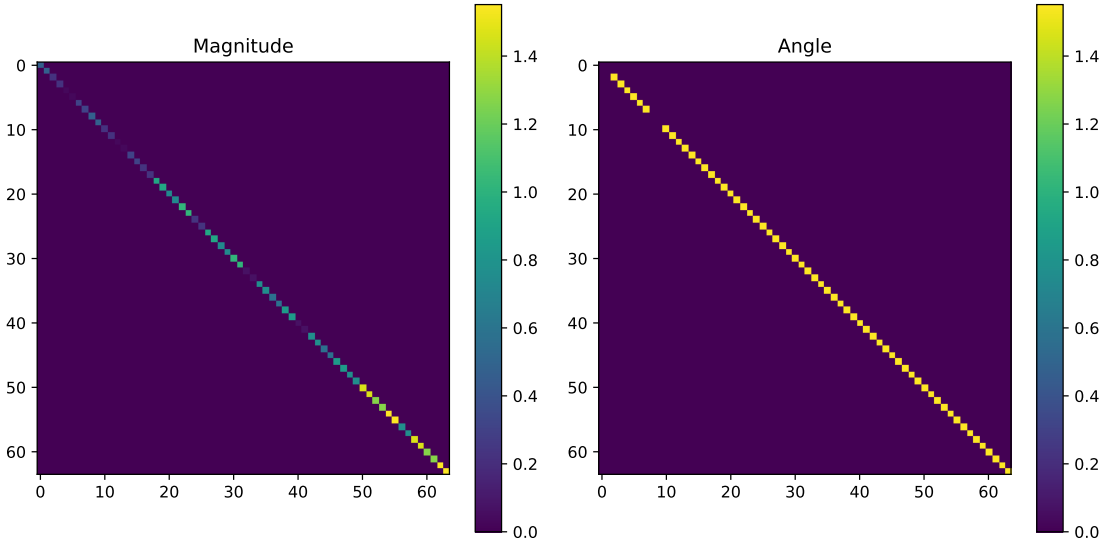


Figure 3.1: Example matrix for  $\hat{H}_{LR} = \hat{H}_L \otimes I^{N_q} + I^{N_q} \otimes \hat{H}_R$  for  $N_m = 6$ .

i.e., where  $p$  represents each combination of  $ijkl$  in lexicographical order. The total number  $N$  of these collections of 4 indices is

$$N = \sum_{i=0}^{d-1} \binom{N_m - i - 1}{3} = \binom{N_m}{4}, \quad (3.3)$$

since for a given  $i$ , we must choose  $j, k, l$  from a set of  $N_m - i - 1$  numbers. Moreover,  $\psi^i, \psi^j, \psi^k, \psi^l$  represent distinct Majorana fermions with a coupling constant  $\mathcal{J}_{ijkl}$ , sampled from a random normal distribution with  $\langle \mathcal{J}_{ijkl} \rangle = 0$  and  $\sigma^2 = \frac{3!J^2}{N_m^3}$  where  $J = 2$  is the effective variance [19] and  $N_m$  is the number of Majorana fermions. We distinguish between the  $L$  and  $R$  subsystems. In order to represent this Hamiltonian on a quantum computer, we must convert the Majorana fermions into qubits. Note that since 1 Majorana converts to 2 qubits, there are  $N_q = N_m/2$  qubits.

We perform this mapping by the Jordan-Wigner encoding given in the supplemental information of [19], which distinguishes between particles coming from the L and R subsystems:

$$\begin{aligned} \psi_L^j &= Z^{\lfloor \frac{j+1}{2} \rfloor} X I^{N_q-2-\lfloor \frac{j+1}{2} \rfloor} \\ \psi_R^j &= Z^{\lfloor \frac{j+1}{2} \rfloor} Y I^{N_q-2-\lfloor \frac{j+1}{2} \rfloor}, \end{aligned} \quad (3.4)$$

where  $X, Y, Z$  are Pauli gates. To be clear, this means each  $\psi$  is a  $2^{N_q} \times 2^{N_q}$  matrix. We then multiply each  $\psi$  together, so the each Pauli string “word” is a  $2^{N_q} \times 2^{N_q}$  matrix. We also considered the alternate mapping given by [13], but chose Equation 3.4 due to its minimal usage of Pauli gates. Note that in this notation, each Majorana  $\psi$  is converted to a “Pauli string” as described in Chapter 1, in which all multiplication is a tensor product. One difference between our definitions and [19] is that we have explicitly included the identities at the ends of the strings they did not include, since otherwise we are adding together strings of different lengths which does not make sense. Figure 3.1 gives an example Hamiltonian using this encoding for  $N_m = 6$ .

### 3.1.2 Time evolution to simplify?

Now that we have a way to convert from Majoranas to qubits via Equation 3.4, we can evaluate Equation 3.2. The number of total terms in equation 3.2 becomes quite large —  $\binom{N_m}{4}$  — so simplification is necessary in order to have any hope of actually running this process on a quantum computer. What [19] did is to interpret  $\mathcal{J}_{ijkl}$  as the weights of a neural network, and then find an optimal set of these parameters such that the resulting mutual information between the input and output registers in the teleportation protocol matches that given by a full SYK Hamiltonian with coefficients from a Gaussian distribution as previously specified. They found the following Hamiltonian:

$$\hat{H}_{L,R} = -0.36\psi^1\psi^2\psi^4\psi^5 + 0.19\psi^1\psi^3\psi^4\psi^7 - 0.71\psi^1\psi^3\psi^5\psi^6 + 0.22\psi^2\psi^3\psi^4\psi^6 + 0.49\psi^2\psi^3\psi^5\psi^7. \quad (3.5)$$

I.e., they were able to set many of the  $\mathcal{J}_{ijkl}$  to 0. Note that here  $N_m = 7$  because in this case [19] indexed from 1. There are several points to observe. As [21] points out, this model is fully commuting, which means that each of the terms in Equation 3.5 commute with the others—a property not by construction characteristic of the SYK model, but in a reply to this comment the original authors [18] prove that commutativity does not influence teleportation. In [18], the authors of the original paper responded to the comment and defended their analysis on several points, including the not-relatedness of full commutativity to teleportation. Even if this feature does not necessarily call into question their results, the comment to the comment does not address a crucial point [21] make, which is that the results of their training procedure does not generalize—a phenomenon known as overfitting.

Therefore, a new way to “compress” SYK Hamiltonians is crucial. To date, as far as we know, no satisfactory alternative has been proposed. We explored how far a simple idea based on converting the Hamiltonian to a quantum circuit via time evolution, which would allow us to use an optimization algorithm to reduce the number of gates required to achieve the same operation. We define the following loss function:

$$L = \|\hat{M} - M\|, \quad (3.6)$$

i.e. the Frobenius norm of the difference of  $\hat{M}$ , the matrix result of the simplified circuit, and  $M$ , the target circuit defined by substituting 3.4 into 3.2. We model this as a `PauliStringOp` object in Qiskit because rather than having to iteratively build an exponential size matrix, we simply concatenate strings and store the  $\mathcal{J}_{ijkl}$  floats and perform operations using these. Specifically, what we considered was to *first* convert the Hamiltonian into a time evolution operator via the Trotter-Suzuki approximation in gate form,

$$e^{-it\hat{H}_{L,R}} \approx \left( \prod_p e^{-it\hat{H}_{pL,R}/n} \right)^n \quad (3.7)$$

using 3.2 and  $n$  is the total number of steps in the time approximation [30]. The clever thing about this approximation is that it allows us to overcome the fact that the terms in the Hamiltonian may not commute. Note that

$$e^{-i\tau X} = R_Y(2\tau), \quad e^{-i\tau Y} = R_Y(2\tau), \quad e^{-i\tau Z} = R_Z(2\tau), \quad (3.8)$$

but we cannot merely tensor product each rotation gate; in order to preserve the interactions between different qubits, we must implement CNOTs. However, it is not a trivial process, as [23] discusses. We use the `PauliEvolutionGate` operator from Qiskit for this purpose.

Figure 3.2 illustrates a sample from the entire wormhole protocol circuit, which is a sinusoidal-looking pattern of CNOTs then rotation gates. The problem with the presence of all these CNOTs is that it is very difficult to simplify the resulting circuit, since unlike an uninterrupted collection of rotation gates which can be reduced to a single 3-axis rotation gate, the CNOTs create conditional breaks in the circuit. This makes the approach we initially considered quite difficult.

However, since the Hamiltonian itself does not contain any conditional logic, theoretically it is possible to compress it—just not as a circuit, since it is not unitary. We implemented both a direct stochastic gradient descent algorithm as well as a Monte Carlo Markov Chain (MCMC) algorithm [14] where the inputs are the  $\mathcal{J}_{ijkl}$ . The

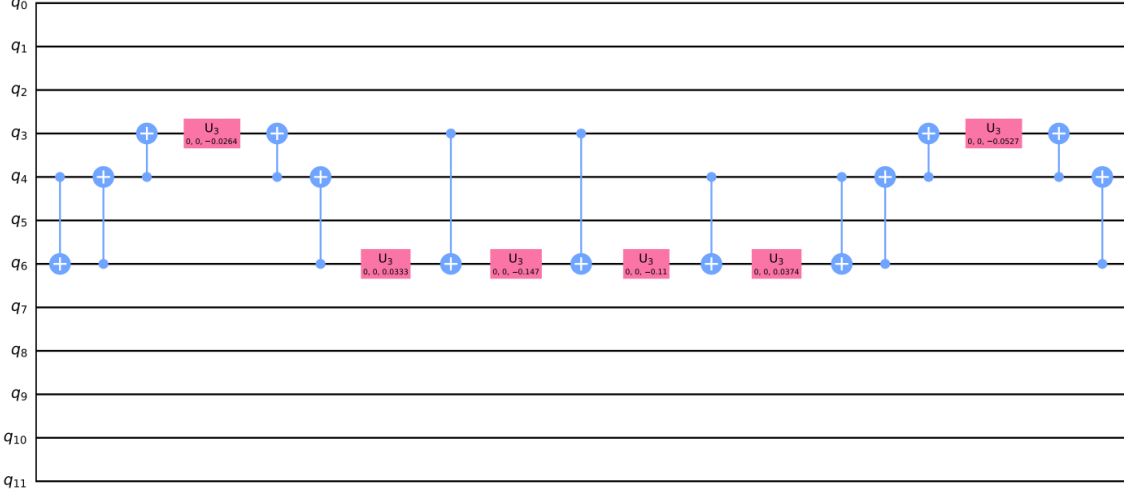


Figure 3.2: Snippet of time evolution circuit on the left part of the wormhole from the protocol.

task is to minimize the Frobenius norm between the predicted Hamiltonian matrix and the actual one. In initial testing, since the matrix must be explicitly calculated in order to measure similarity, gradient descent is too slow, which is why an optimized guessing algorithm like MCMC holds more promise. That said, I have not yet extensively optimized or tested this approach since, as will be explained, the simulation environment itself has not been completely validated.

## 3.2 Implementation of rest of wormhole protocol

We will proceed with defining the rest of the wormhole protocol. The backbone of the protocol is the ‘‘thermofield double state’’, which represents the two entangled black holes. Mathematically,

$$|\text{TFD}\rangle = e^{\hat{H}\beta} |n\rangle_L |n\rangle_R, \quad (3.9)$$

where we dedicate  $N_q$  qubits to the L black hole and the same number to the right for a total register of  $2N_q = N_m$  qubits. [19] in their Supplemental Information discusses that implementing a Variational Quantum Eigensolver (VQE) on the combined Hamiltonian below will approximately prepare the TFD of inverse temperature  $\beta = \frac{1}{k_B T}$  where  $k_B$  is Boltzmann’s constant with potential  $V$ , by [8]:

$$\hat{H}_{\text{TFD}} = \hat{H}_L + \hat{H}_R + i\beta\hat{V} \quad (3.10)$$

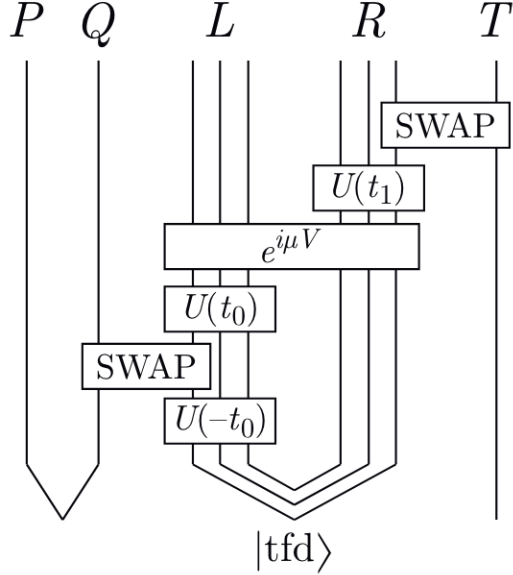


Figure 3.3: Wormhole protocol circuit implementation, courtesy of [19]

Note the authors assume  $\beta = 4$ . Although not explicitly specified by [19], we assume  $H_L$  contains an implicit identity at the end of each of the terms in the Pauli strings of length  $N_q$  and at the beginning of  $H_R$  in order that the L Hamiltonian acts only on the left subsystem and the R Hamiltonian only acts on the right. This ensures that the sum is valid, since  $V$  is defined to act on both subsystems. In particular, the potential  $V$  is defined as:

$$\hat{V} = \frac{1}{4N_m} \sum_{j=0}^{N_m-1} \psi_L^j \psi_R^j. \quad (3.11)$$

The idea of VQE is to set up a preset parametrized circuit, and then find the parameters such that the resultant minimum energy most closely matches the actual lowest energy of  $H_{TFD}$ . However, the authors do not specify what the ansatz should be, except to say they used  $2N_m - 1$  conditional gates. We tried 4 configurations,

0. `EfficientSU2` from Qiskit, which is 2 series of CNOTs and single qubit rotations,
1. an initial layer of single qubit rotation gates followed by a chain of CNOTs with additional rotation gates,

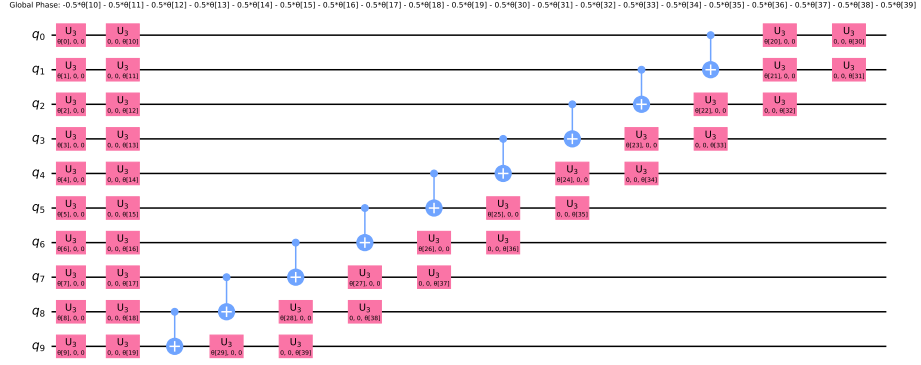


Figure 3.4: Ansatz 0

2. like (1) but with a CNOT chain on the L,
3. like (2), but CNOT chain applied to L and R

Ansatzes 0-3 are shown in Figure 3.4 to 3.7.

Ansatz	Mean	SEM
0	0.2	0.1
1	0.3	0.1
2	0.2	0.1
3	0.4	0.2

Table 3.1: Relative error of ground state energies for 100 repetitions, defined by Equation 3.12, computing both the mean and standard error of the mean.

We performed VQE in Qiskit to determine the optimal parameters, and then compared the minimal eigenvalue of the VQE to the actual given by the `NumPyMinimumEigensolver` algorithm by measuring the absolute relative error, defined as

$$e_r = \frac{|\hat{E}_0 - E_0|}{|E_0|}, \quad (3.12)$$

where  $E_0$  is the “true” ground state energy and  $\hat{E}_0$  is that estimated by VQE. Table 3.1 shows the results for 100 repetitions. We use both `SPCA` and `L_BFGS_B` optimizers, but the benchmark results quoted here are for the former.

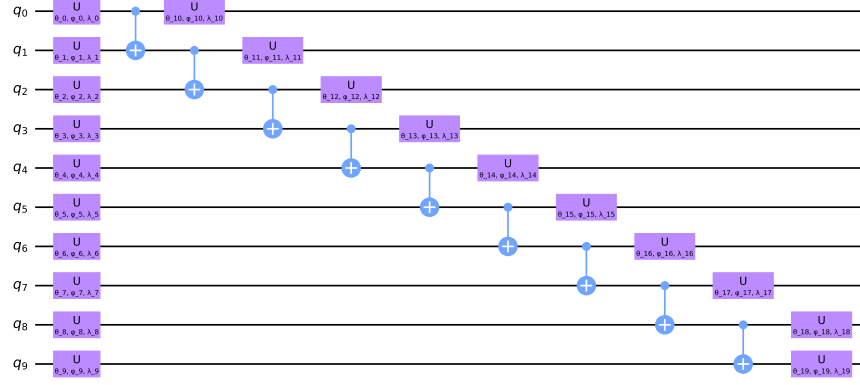


Figure 3.5: Ansatz 1

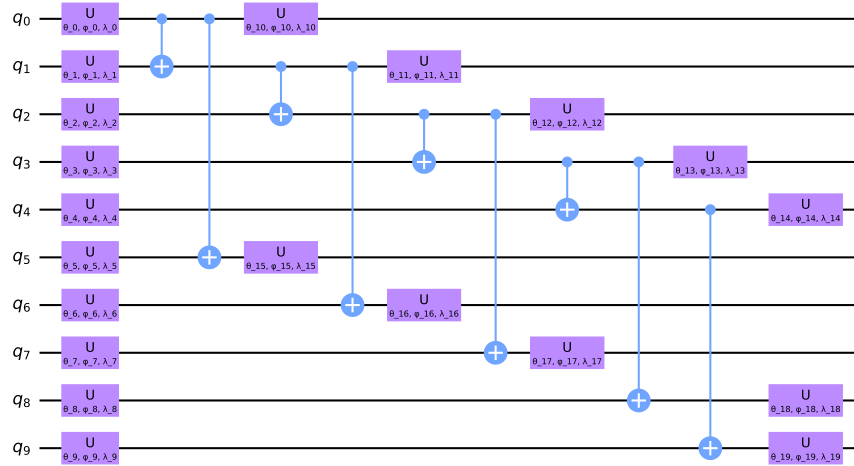


Figure 3.6: Ansatz 2

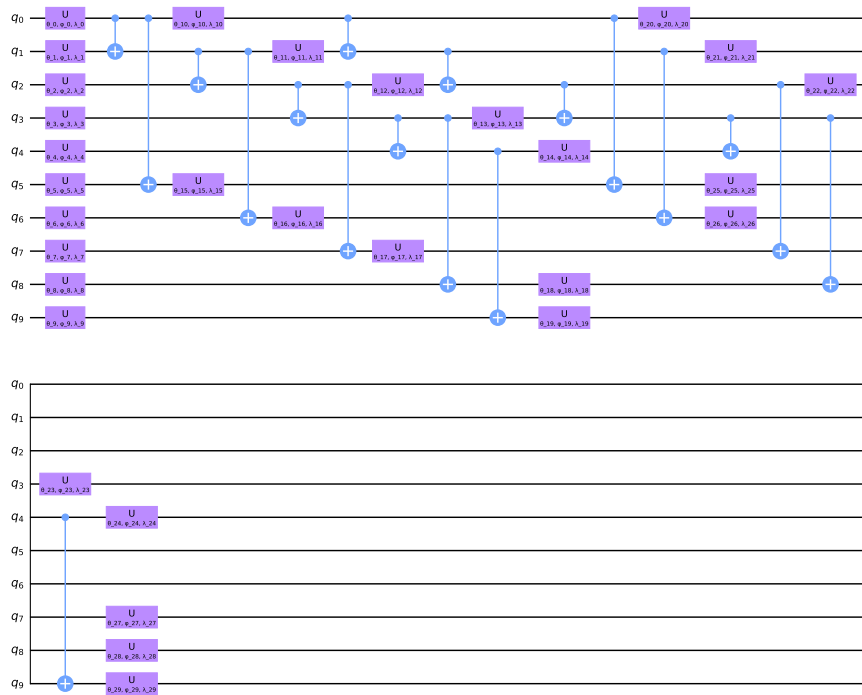


Figure 3.7: Ansatz 3

Note that Ansatz 0, the `EfficientSU2` performs the best, but the relative error is still quite high—this suggests that we have not found the truly optimal VQE ansatz. Moreover, as the first column of mutual information simulations in Figure 3.8 reveal, only Ansatz 0 has no mutual information transmitted for  $\mu = 0$ , making it the only plausible ansatz of the four.

To continue building up the simulation, we apply Equation 3.8 on  $\hat{H}_L$  to implement time evolution to a time  $-t_0$  for  $t_0 = 2.8$  to contract the wormhole for optimal teleportation. Then, we insert an entangled Bell state  $|\phi^+\rangle = \frac{1}{\sqrt{2}}(|00\rangle + |11\rangle)$  “into the wormhole” by performing a SWAP operation to the second qubit of the Bell state and the first qubit of the L subsystem. The left qubit of the Bell state we call  $P$ . [19] and [13] state that this SWAP gate is actually equivalent to the normal SWAP gate, so we can directly apply this operation. Then we apply another time evolution on the L subsystem, now by  $+t_0$  to expand the wormhole. We then apply a coupling operator to the two subsystems  $e^{i\mu V}$  implemented via Trotter-Suzuki for  $\mu = -12$ , which should induce an asymmetric teleportation signal. Next, we time evolve the R subsystem by a variable amount  $t$ . Finally, we can perform our measurement of “teleportation signal”: how much information is shared between P and the last qubit  $T$  of the R subsystem of the TFD?

Specifically, we measure the mutual information of the first and last qubits in the combined circuit. We define  $\rho_P$ ,  $\rho_T$ , and  $\rho_{PT}$  as the reduced density matrices of qubits P, T, and the combined system PT respectively. We obtain these matrices by performing a partial state tomography, or reconstruction, on subsystems P and T, and then trace out P or T to create the reduced density matrices, just as explained below Equation 1.46. We use Qiskit’s `StateTomography` experiment which allows us to select the qubits of interest from the start so we do not have to measure the entire circuit, and the function `entropy` which automatically computes the Von Neumann entropy.

We assume  $N_m = 10$  since [19] claims that this value is high enough to generate wormhole teleportation but not too large to be computationally infeasible. Figure 3.8 gives the results of the wormhole simulation for several conditions. Each row gives a particular ansatz, and each column represents a  $\mu$  coupling constant. To be a physical simulation, we need  $I = 0$  for  $\mu = 0$ . Looking at the middle column, we can immediately rule out all ansatzes except for ansatz 0 (note the scale of  $10^{-15}$  there). However, if we look then at the first column and first row, we see that the shape is not constant: there are some (the brown and purple) that look approximately correct, but there are many more others that either appear constant or have an inverted shape. Figure 3.9 gives the normalized results of each run to

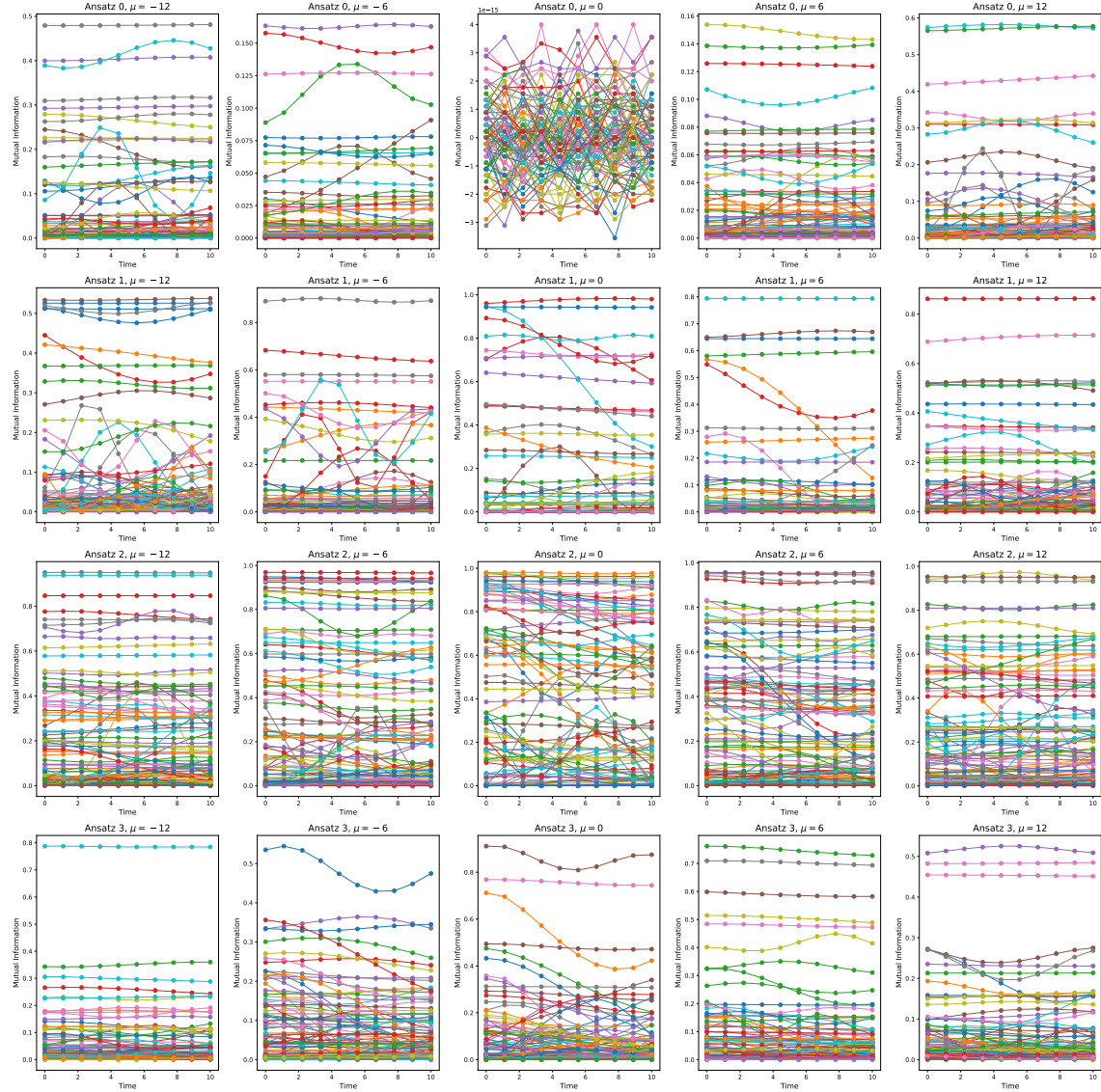


Figure 3.8: Results of  $I_{PT}$  as a function of time  $t$  plotted for each Ansatz and each  $\mu$ , running the simulation multiple times.

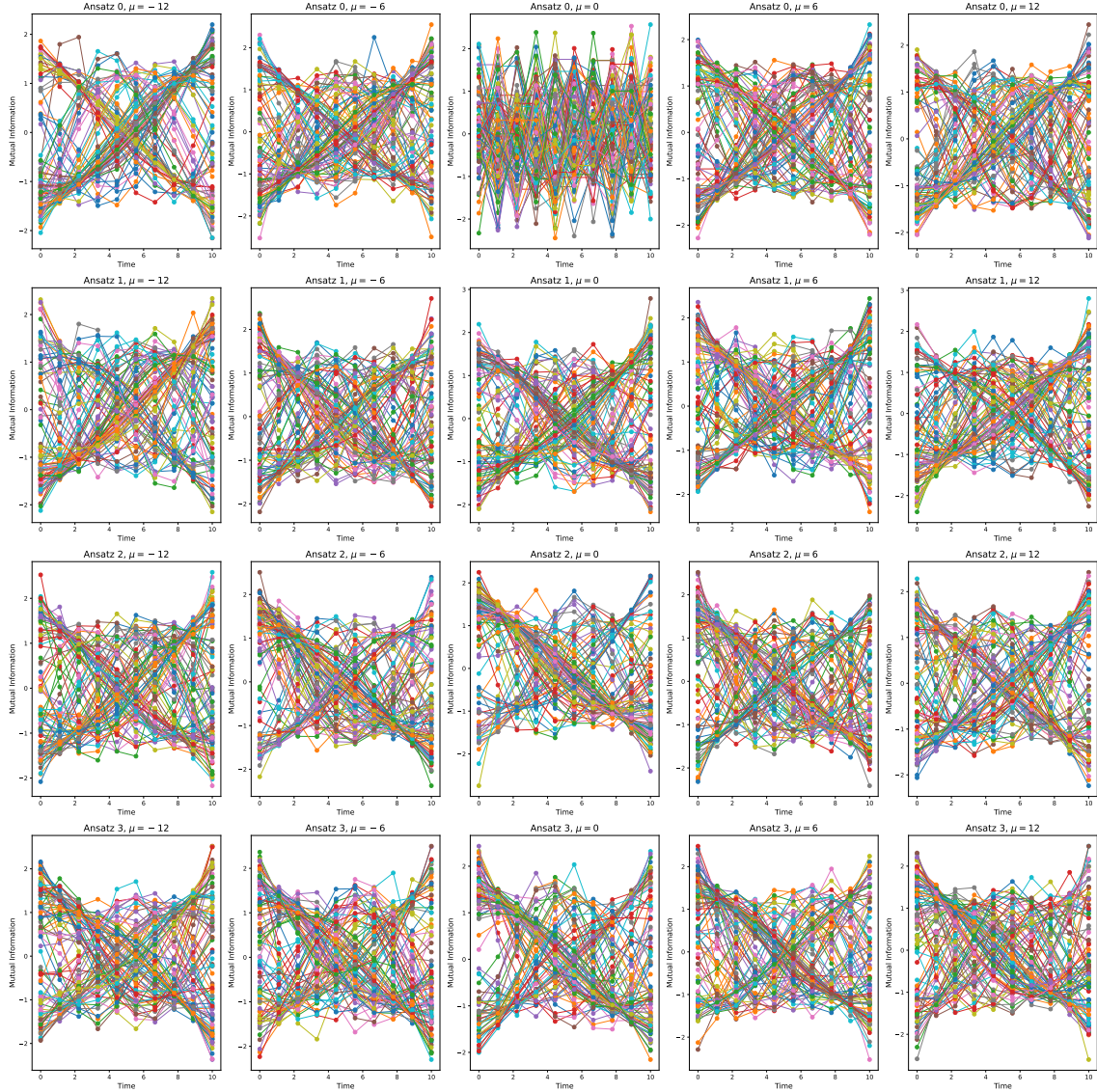


Figure 3.9: Standardizing the results of the simulations in Figure 3.8 so we can compare the overall shape of each run.

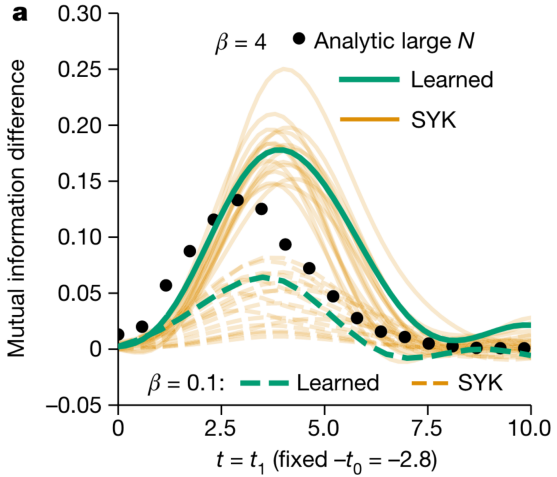


Figure 3.10: Snapshot of Figure 3a from [19] showing mutual information difference for  $I_{\mu<0} - I_{\mu>0}$ . While this is not a plot of mutual information but rather the difference between two plots of mutual information (for a plot of mutual information directly, see Figure 3.11), this plot has several advantages: first, the overall shape is the same as for the mutual information itself, so we can use it to make a qualitative comparison, and second it includes an exact solution for large  $N$ , shown as black dots. This is the training data for the parametrized circuit gedankenexperiment of section 3.3.

allow for easier multi-run comparison. We see many “X”-like graphs, which indicates a variety of simulations that have both the correct asymmetry and reversed direction of asymmetry.

In Figure 3.10, we can see what we should expect to see, which is an asymmetric *peak* clustered around lower time values. We expect there to be slight differences in the shapes of the mutual information curves since the coefficients of  $\hat{H}$  are random, but it is not clear to us whether this level of variation is acceptable, in particular if *every* SYK simulation should yield that asymmetric peak or if only some subset of those—but if so, then according to what conditions? Moreover, these circuits require 12 qubits, 333 CNOT gates, and 171 3-axis rotation gates which is prohibitive to actual experimental implementation.

As a final validation of the circuit simulation protocol, we coded the learned Hamiltonian given in Equation 3.5 and ran wormhole teleportation using Ansatz 0, which yielded the plot shown in Figure 3.12. As we see, the change in mutual information is quite small and does not match the maximum value of 0.25 as in [19], reproduced

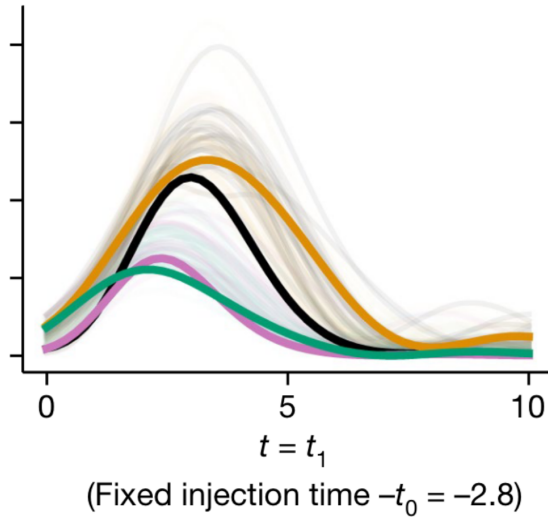


Figure 3.11: Mutual information for the SYK curves highlighting the Hamiltonian of Equation 3.5. The black curve represents the full simulated Hamiltonian before sparsification for  $\mu = -12$ , then in pink for  $\mu = +12$ . In orange, they plot the sparsified version, which is Equation 3.5, for  $\mu = -12$ , and in pink they plot  $\mu = +12$ . The  $y$ -axis scale is from 0 to 0.4, evenly spaced.

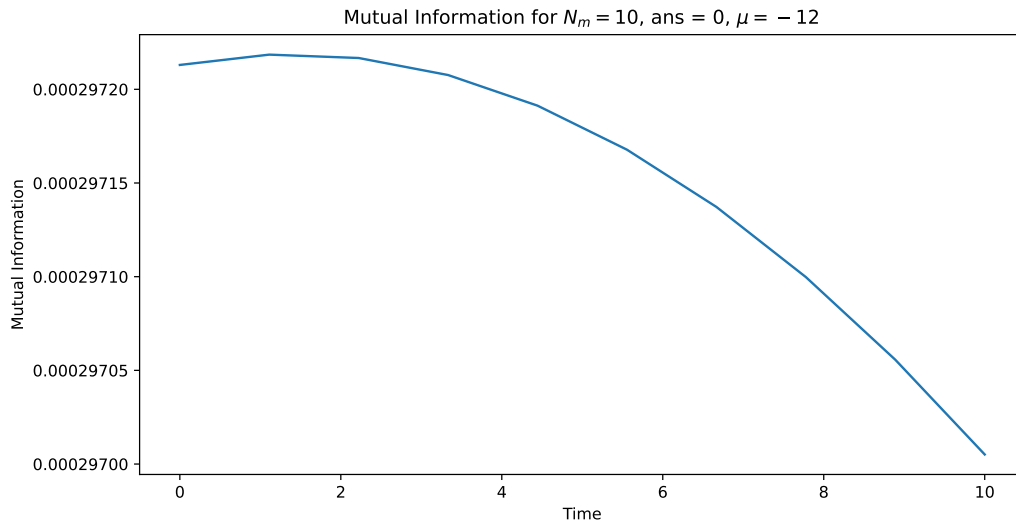


Figure 3.12: Simulation of the Hamiltonian in equation 3.5 using  $\mu = -12$  with my code. Compare to Figure 3.11.

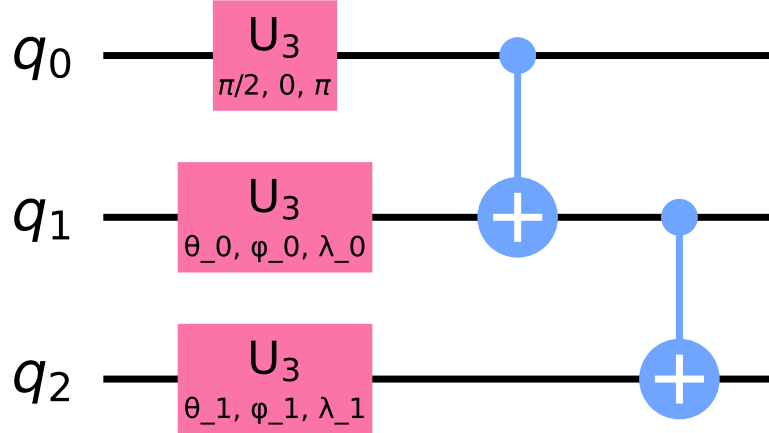


Figure 3.13: Proposed ansatz for the mutual information reconstruction.

in Figure 3.11. It is clear our simulation is inconsistent with the expected results. Most likely the issue is due to not choosing the correct VQE as our work earlier in this chapter showed.

### 3.3 An experiment with a philosophical question

Faced with these unfavorable simulation results, we decided to perform an experiment. What if I define a very simple 3-qubit circuit as in Figure 3.13, which has a Hadamard gate on the first qubit, then a 3-axis rotation gate for each remaining qubit and CNOTs between them, and leave the 6 rotation angles as parameters. Then, I try to match the mutual information values in 3.10 by finding the optimal parameters for each mutual information value through gradient descent? I defined a loss function

$$L = |\hat{I}_{PT} - I_{PT}|, \quad (3.13)$$

where  $I_{PT}$  is the actual mutual information value extracted from the “analytic solution for large  $N$ ” from Figure 3.10 and  $\hat{I}_{PT}$  is the predicted mutual information

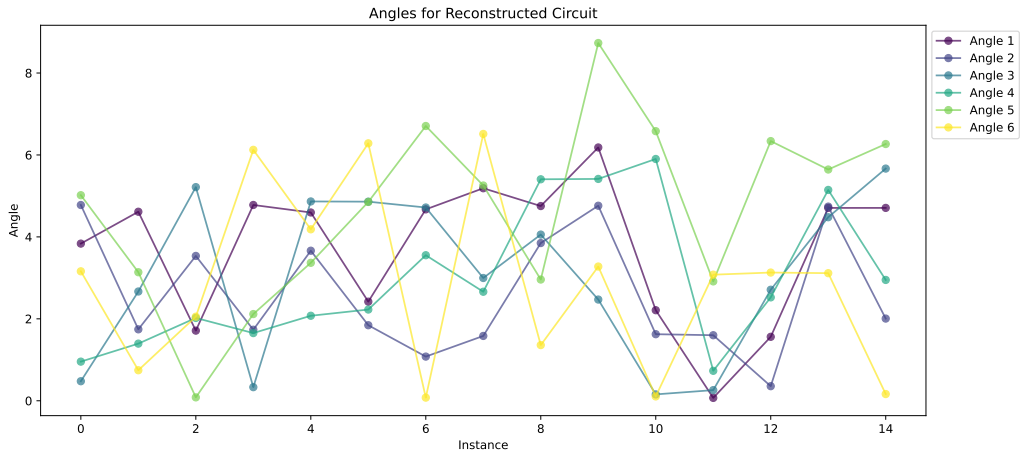


Figure 3.14: Plot of the angles in Figure 3.13 for each iteration.

given the configuration of the angles. We chose the analytic solution for large  $N$  because they were clearly defined points and even though technically it might have more physical sense to choose data from Figure 2b in [19] since that comes from  $\mu = -12$ , the authors throughout the paper stress the shape of the peak more than the particular values of mutual information, such as with their learned Hamiltonians, which supports this decision. Using 15 datapoints, the result from the gradient descent, implemented via my custom SGD package `trabbit`, yields an average loss of  $1.0 \times 10^{-9} \pm 0.3 \times 10^{-9}$ .

The relationship between the learned angles and which datapoint they correspond to is shown in Figure 3.14, which reveals approximately sinusoidal behavior. It would be interesting to consider if there exists an analytic relationship between each of the rotation angles and the time  $t$  parameter of the experiment. To validate the results of the optimization, we perform simulation with noise to mimic real quantum devices via the `ibmq_qasm_simulator` backend from the `IBMQ` provider, using 10000 shots repeated 5 times to obtain the average and SEM. The result is shown in Figure 3.15, where the “Actual” results are from [19] and the “Reconstructed” are from the noisy simulation, which align closely suggesting successful learning even in spite of noise.

We have also run the same experiment but with 2000 shots on the 127 qubit Kyoto Eagle processor (`ibm_kyoto` backend), in order to obtain data from actual quantum hardware to compare performance to the theoretical and noisy simulated results. We see that while overall the noisy simulated results agree quite well with the dynam-

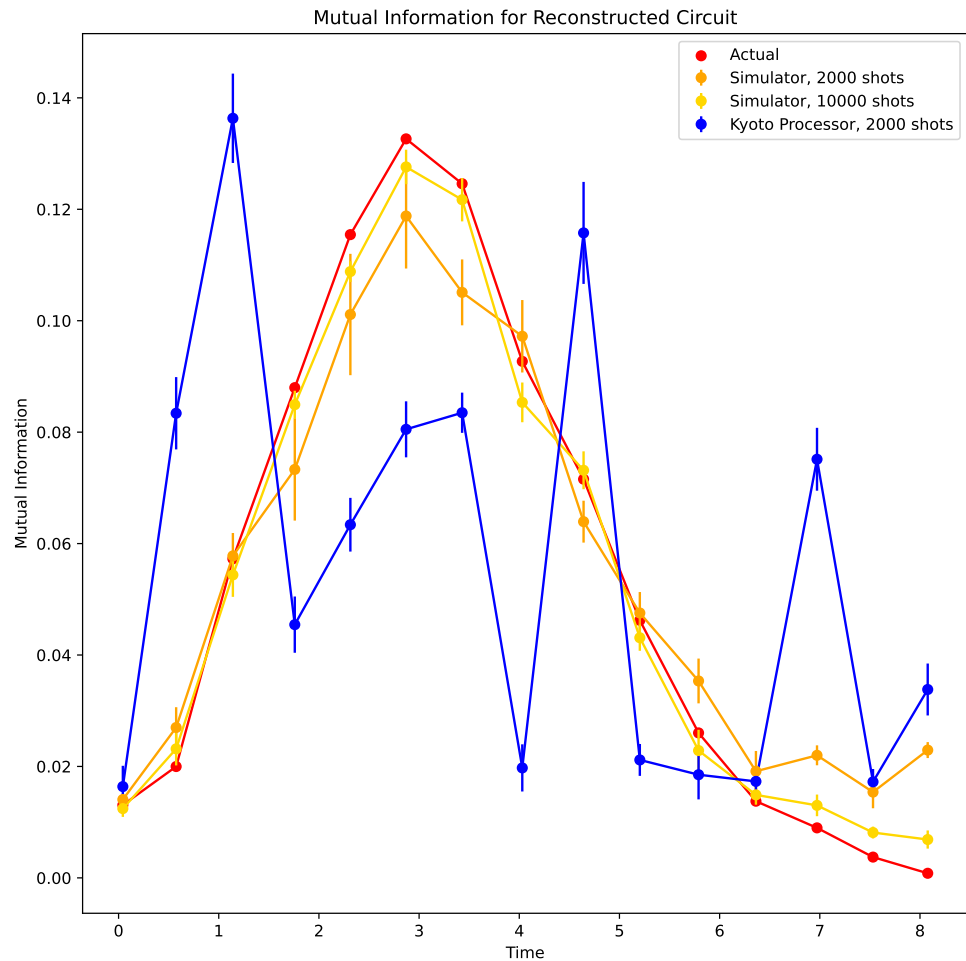


Figure 3.15: Mutual information comparison of theoretical and noisy simulations with Qiskit.

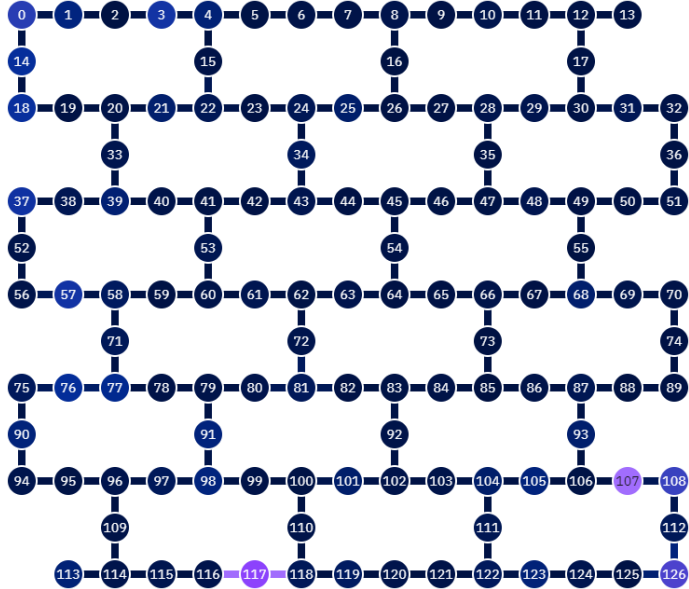


Figure 3.16: Calibration data for each of the qubits in the IBM Eagle processor Kyoto, where each qubit is colored by ECR error where darker is better.

ics we are trying to capture, the real quantum data is quite literally all over the place. That said, there is a clear relationship that the mutual information begins small, grows large in the middle, and then ends small again—so qualitatively, this is what we want to see. However, it is very unstable in the middle. This reflects the reality that current quantum processors do not have in-built error correction. It is possible to error *mitigate*, which are post-measurement operations—this is a current area of research for the project, because there is no native way to error mitigate a StateTomography experiment, as of Qiskit in Spring 2024 to my knowledge.

Figure 3.16 gives a map of the qubit connectedness colored by gate error, which is part of an hourly calibration routine performed by IBM. Note that while the original Ansatz has 5 gates (1 Hadamard, 2 3-axis rotation, and 2 CNOT), the Eagle processors work in the  $R_Z$ ,  $S_X$ , ECR, and  $X$  basis. ECR refers to Echoed Cross-Resonance, which is a 2-qubit conditional gate that operates physically by driving the control qubit at the resonant frequency of the target by a microwave pulse, and  $S_X = \sqrt{X}$  is a rotation by  $\frac{\pi}{2}$  as explained in Equations 1.53, 1.54, 1.41, 1.36. In this basis, 23 total gates are required: 12  $R_Z$ , 7  $S_X$ , 2 ECR, and 2  $X$ . Each simulation takes 6 seconds to execute, including measurement and partial state reconstruction for 2000 shots, and total time from request submission to queue completion is approximately 10 minutes.

More detailed properties of Kyoto are given in Table 3.2. We note that anyone can register for an IBM Quantum Platform account for free, and included in that is 10 minutes of compute (not counting queue time) on real hardware per month, so all computations were free (simulations are of course free, and Qiskit itself is free).

Metric	Value
Median ECR error	$9.421 \times 10^{-3}$
Median SX error	$2.941 \times 10^{-4}$
Median readout error	$1.420 \times 10^{-2}$
Median T1	$220.24 \mu s$
Median T2	$106.28 \mu s$

Table 3.2: IBM Kyoto Performance Metrics, from IBM. T1 and T2 refer to coherence times, which quantify how long a quantum state retains its “quantumness” before decohering after a too great amount of interaction.

We have demonstrated that this simple ansatz can learn intricate mutual information dynamics and is resistant to simulated noise, we ask what it is we really accomplished. On the one hand, we have not really implemented the wormhole protocol as described in the previous section in that we cannot interpret any part of this ansatz as the L black hole or the R black hole, with time evolution operators according to this particular Hamiltonian. Yet, the result is the same but with a tiny fraction of the computational cost. Therefore, we believe that a valid strategy for simulation with NISQ devices may be that instead of focusing on a direct translation of theoretical continuous operators to physical discrete ones, we can instead focus on the results—which is what we actually care about. Our plan would be to generate a set of training data of mutual information as a function of time  $t$  in order to generate new sets of input angles to the ansatz of this section and determine if those angles produce meaningful new mutual information curves. If so, then we will have demonstrated that this ansatz can not only be optimized to a particular curve, but can capture the information aspect of the SYK wormhole teleportation dynamics. We could also extend this to other measures, like time correlation and size winding, and see how well these learned circuits can generate meaningful values. This could be a new strategy to implementing more complex quantum simulations on NISQ devices with a feasible number of qubits and gates.

# Bibliography

- [1] Atchade Parfait Adelomou, Elisabet Golobardes Ribe, and Xavier Vilasis Cardona. *Using the Parameterized Quantum Circuit combined with Variational-Quantum-Eigensolver (VQE) to create an Intelligent social workers' schedule problem solver*. Oct. 2020. DOI: 10.48550/arXiv.2010.05863. URL: <http://arxiv.org/abs/2010.05863> (visited on 03/26/2024).
- [2] Jason Alicea. "New directions in the pursuit of Majorana fermions in solid state systems". en. In: *Reports on Progress in Physics* 75.7 (June 2012), p. 076501. ISSN: 0034-4885. DOI: 10.1088/0034-4885/75/7/076501. URL: <https://dx.doi.org/10.1088/0034-4885/75/7/076501> (visited on 09/16/2023).
- [3] Alain Aspect, Philippe Grangier, and Gérard Roger. "Experimental Realization of Einstein-Podolsky-Rosen-Bohm Gedankenexperiment: A New Violation of Bell's Inequalities". In: *Physical Review Letters* 49.2 (July 1982), pp. 91–94. DOI: 10.1103/PhysRevLett.49.91. URL: <https://link.aps.org/doi/10.1103/PhysRevLett.49.91> (visited on 03/20/2024).
- [4] Angelo Bassi et al. "Models of wave-function collapse, underlying theories, and experimental tests". In: *Reviews of Modern Physics* 85.2 (Apr. 2013), pp. 471–527. DOI: 10.1103/RevModPhys.85.471. URL: <https://link.aps.org/doi/10.1103/RevModPhys.85.471> (visited on 04/10/2024).
- [5] J. S. Bell. "On the Einstein Podolsky Rosen paradox". en. In: *Physics Physique Fizika* 1.3 (Nov. 1964), pp. 195–200. ISSN: 0554-128X. DOI: 10.1103/PhysicsPhysiqueFizika.1.195. URL: <https://link.aps.org/doi/10.1103/PhysicsPhysiqueFizika.1.195> (visited on 03/19/2024).
- [6] Paul Benioff. "The computer as a physical system: A microscopic quantum mechanical Hamiltonian model of computers as represented by Turing machines". en. In: *Journal of Statistical Physics* 22.5 (May 1980), pp. 563–591. ISSN: 1572-9613. DOI: 10.1007/BF01011339. URL: <https://doi.org/10.1007/BF01011339> (visited on 02/24/2024).

- [7] M. Cerezo et al. “Variational Quantum Algorithms”. In: *Nature Reviews Physics* 3.9 (Aug. 2021), pp. 625–644. ISSN: 2522-5820. DOI: 10.1038/s42254-021-00348-9. URL: <http://arxiv.org/abs/2012.09265> (visited on 03/26/2024).
- [8] William Cottrell et al. “How to Build the Thermofield Double State”. In: *Journal of High Energy Physics* 2019.2 (Feb. 2019), p. 58. ISSN: 1029-8479. DOI: 10.1007/JHEP02(2019)058. URL: <http://arxiv.org/abs/1811.11528> (visited on 08/31/2023).
- [9] D. Deutsch, A. Barenco, and A. Ekert. “Universality in Quantum Computation”. In: *Proceedings of the Royal Society of London. Series A: Mathematical and Physical Sciences* 449.1937 (June 1995), pp. 669–677. ISSN: 0962-8444, 2053-9177. DOI: 10.1098/rspa.1995.0065. URL: <http://arxiv.org/abs/quant-ph/9505018> (visited on 03/26/2024).
- [10] David Deutsch and Roger Penrose. “Quantum theory, the Church–Turing principle and the universal quantum computer”. In: *Proceedings of the Royal Society of London. A. Mathematical and Physical Sciences* 400.1818 (Jan. 1997), pp. 97–117. DOI: 10.1098/rspa.1985.0070. URL: <https://royalsocietypublishing.org/doi/abs/10.1098/rspa.1985.0070> (visited on 02/23/2024).
- [11] A. Einstein, B. Podolsky, and N. Rosen. “Can Quantum-Mechanical Description of Physical Reality Be Considered Complete?” In: *Physical Review* 47.10 (May 1935), pp. 777–780. DOI: 10.1103/PhysRev.47.777. URL: <https://link.aps.org/doi/10.1103/PhysRev.47.777> (visited on 03/20/2024).
- [12] Dmitry A. Fedorov et al. “VQE method: a short survey and recent developments”. en. In: *Materials Theory* 6.1 (Jan. 2022), p. 2. ISSN: 2509-8012. DOI: 10.1186/s41313-021-00032-6. URL: <https://doi.org/10.1186/s41313-021-00032-6> (visited on 03/26/2024).
- [13] Ping Gao and Daniel Louis Jafferis. “A traversable wormhole teleportation protocol in the SYK model”. en. In: *Journal of High Energy Physics* 2021.7 (July 2021), p. 97. ISSN: 1029-8479. DOI: 10.1007/JHEP07(2021)097. URL: [https://doi.org/10.1007/JHEP07\(2021\)097](https://doi.org/10.1007/JHEP07(2021)097) (visited on 10/27/2023).
- [14] Charles J. Geyer. “Practical Markov Chain Monte Carlo”. In: *Statistical Science* 7.4 (1992), pp. 473–483. ISSN: 0883-4237. URL: <https://www.jstor.org/stable/2246094> (visited on 04/11/2024).
- [15] Laszlo Gyongyosi and Sandor Imre. “A Survey on quantum computing technology”. In: *Computer Science Review* 31 (Feb. 2019), pp. 51–71. ISSN: 1574-0137. DOI: 10.1016/j.cosrev.2018.11.002. URL: <https://www.sciencedirect.com/science/article/pii/S1574013718301709> (visited on 03/26/2024).

- [16] Petr Hajicek. “Origin of Hawking radiation”. In: *Physical Review D* 36.4 (Aug. 1987), pp. 1065–1079. DOI: 10.1103/PhysRevD.36.1065. URL: <https://link.aps.org/doi/10.1103/PhysRevD.36.1065> (visited on 04/11/2024).
- [17] Veronika E. Hubeny. “The AdS/CFT Correspondence”. In: *Classical and Quantum Gravity* 32.12 (June 2015), p. 124010. ISSN: 0264-9381, 1361-6382. DOI: 10.1088/0264-9381/32/12/124010. URL: <http://arxiv.org/abs/1501.00007> (visited on 09/14/2023).
- [18] Daniel Jafferis et al. *Comment on "Comment on "Traversable wormhole dynamics on a quantum processor"*”. Mar. 2023. URL: <http://arxiv.org/abs/2303.15423> (visited on 04/02/2024).
- [19] Daniel Jafferis et al. “Traversable wormhole dynamics on a quantum processor”. en. In: *Nature* 612.7938 (Dec. 2022), pp. 51–55. ISSN: 1476-4687. DOI: 10.1038/s41586-022-05424-3. URL: <https://www.nature.com/articles/s41586-022-05424-3> (visited on 06/14/2023).
- [20] J. Keski-Rahkonen et al. “Quantum Lissajous Scars”. In: *Physical Review Letters* 123.21 (Nov. 2019), p. 214101. DOI: 10.1103/PhysRevLett.123.214101. URL: <https://link.aps.org/doi/10.1103/PhysRevLett.123.214101> (visited on 03/26/2024).
- [21] Bryce Kobern, Thomas Schuster, and Norman Y. Yao. *Comment on "Traversable wormhole dynamics on a quantum processor"*. Feb. 2023. DOI: 10.48550/arXiv.2302.07897. URL: <http://arxiv.org/abs/2302.07897> (visited on 06/14/2023).
- [22] Pieter Kok. *2: The Postulates of Quantum Mechanics*. en. Nov. 2021. URL: [https://phys.libretexts.org/Bookshelves/Quantum\\_Mechanics/Advanced\\_Quantum\\_Mechanics\\_\(Kok\)/02%3A\\_The\\_Postulates\\_of\\_Quantum\\_Mechanics](https://phys.libretexts.org/Bookshelves/Quantum_Mechanics/Advanced_Quantum_Mechanics_(Kok)/02%3A_The_Postulates_of_Quantum_Mechanics) (visited on 03/19/2024).
- [23] Gushu Li et al. *Paulihedral: A Generalized Block-Wise Compiler Optimization Framework For Quantum Simulation Kernels*. Sept. 2021. DOI: 10.48550/arXiv.2109.03371. URL: <http://arxiv.org/abs/2109.03371> (visited on 02/20/2024).
- [24] Tianlin Li et al. “Supersymmetric SYK model and random matrix theory”. In: *Journal of High Energy Physics* 2017.6 (June 2017), p. 111. ISSN: 1029-8479. DOI: 10.1007/JHEP06(2017)111. URL: <http://arxiv.org/abs/1702.01738> (visited on 08/19/2023).
- [25] Juan Maldacena and Douglas Stanford. “Remarks on the Sachdev-Ye-Kitaev model”. In: *Physical Review D* 94.10 (Nov. 2016), p. 106002. DOI: 10.1103/PhysRevD.94.106002. URL: <https://link.aps.org/doi/10.1103/PhysRevD.94.106002> (visited on 07/21/2023).

- [26] Isaac L. Chuang Michael A. Nielsen. *Quantum Computation And Quantum Information 10th Anniversary Edition*. eng. June 2012. URL: <http://archive.org/details/QuantumComputationAndQuantumInformation10thAnniversaryEdition> (visited on 03/20/2024).
- [27] Michael E. Peskin. *An Introduction To Quantum Field Theory*. Boca Raton: CRC Press, Jan. 2018. ISBN: 978-0-429-50355-9.
- [28] John Preskill. *Quantum computing 40 years later*. Feb. 2023. URL: <http://arxiv.org/abs/2106.10522> (visited on 02/23/2024).
- [29] M. Robnik. “Fundamental concepts of quantum chaos”. en. In: *The European Physical Journal Special Topics* 225.6 (Sept. 2016), pp. 959–976. ISSN: 1951-6401. DOI: 10.1140/epjst/e2016-02649-0. URL: <https://doi.org/10.1140/epjst/e2016-02649-0> (visited on 03/26/2024).
- [30] Masuo Suzuki. “Improved Trotter-like formula”. In: *Physics Letters A* 180.3 (Sept. 1993), pp. 232–234. ISSN: 0375-9601. DOI: 10.1016/0375-9601(93)90701-Z. URL: <https://www.sciencedirect.com/science/article/pii/037596019390701Z> (visited on 02/20/2024).
- [31] John Townsend. *A Modern Approach to Quantum Mechanics*. en. University Science Books, July 2012. ISBN: 978-1-891389-78-8.
- [32] M. Vázquez and Arnold Hanslmeier. *Ultraviolet Radiation in the Solar System*. en. Springer Science & Business Media, Dec. 2005. ISBN: 978-1-4020-3726-9.
- [33] Juan Yin et al. “Satellite-based entanglement distribution over 1200 kilometers”. In: *Science* 356.6343 (June 2017), pp. 1140–1144. DOI: 10.1126/science.aan3211. URL: <https://www.science.org/doi/full/10.1126/science.aan3211> (visited on 03/20/2024).